



Salla Hiltunen

HYDROTHERMAL STABILITY OF MICROFIBRILLATED CELLULOSE



Salla Hiltunen

HYDROTHERMAL STABILITY OF MICROFIBRILLATED CELLULOSE

Dissertation for the degree of Doctor of Science (Technology) to be presented with due permission for public examination and criticism in the Auditorium of the Student Union House at Lappeenranta-Lahti University of Technology LUT, Lappeenranta, Finland on the 6th of September, 2019, at noon.

Acta Universitatis
Lappeenrantaensis 865

Supervisor Docent Kaj Backfolk
LUT School of Energy Systems
Lappeenranta-Lahti University of Technology LUT
Finland

Reviewers Professor Raimo Alén
Department of Chemistry
University of Jyväskylä
Finland

Professor Ulf Germgård
Department of Engineering and Chemical Sciences
Karlstad University
Sweden

Opponent Associate Professor Henrikki Liimatainen
Fibre and Particle Engineering Research Unit
University of Oulu
Finland

ISBN 978-952-335-401-2
ISBN 978-952-335-402-9 (PDF)
ISSN-L 1456-4491
ISSN 1456-4491

Lappeenranta-Lahti University of Technology LUT
LUT University Press 2019

Abstract

Salla Hiltunen

Hydrothermal stability of microfibrillated cellulose

Lappeenranta 2019

76 pages

Acta Universitatis Lappeenrantaensis 865

Diss. Lappeenranta-Lahti University of Technology LUT

ISBN 978-952-335-401-2, ISBN 978-952-335-402-9 (PDF), ISSN-L 1456-4491, ISSN 1456-4491

The aim of this study was to investigate the effects of hydrothermal treatment on microfibrillated cellulose (MFC). MFC gels were prepared by fibrillating never-dried kraft and dissolving pulps pretreated with endoglucanase. The MFC gels were then exposed to hydrothermal treatment in batch experiments for different times at different temperatures. A comparative experiment was made with a sodium carboxymethyl cellulose (NaCMC) solution in order to reveal possible differences in behavior of these two materials after exposure to hydrothermal treatment. The NaCMC suspensions were further tested with MFC in a different hydrothermal treatment mode consisting of a short-term thermal treatment with steam. The effects of temperature and treatment time on the gel viscosity, viscoelastic (G' and G'') behavior of the MFC, and on its water retention and surface charge were measured, and the low molar mass degradation products from the filtrates were determined.

It was found that hydrothermal treatment under batch conditions affected the MFC gel structure by reducing its water retention capacity. The viscosity of the gels was also reduced to an extent that depended on the MFC grade used. The pH of the gels also decreased, indicating the formation of acidic compounds. Analysis of the hydrolysis products revealed that the filtrates contained a complex mixture of different degradation products, some of them only in trace amounts, and some components remained unknown. The main hydrolysis products formed were sugars and numerous carboxylic acids. Hydrothermal treatment also led to an increase in the UV/VIS absorption of the gels indicating the presence of chromophores.

The NaCMC solutions were sensitive to hydrothermal treatment, as the viscosity of NaCMC solutions decreased already after a brief steam treatments. Short-term steam treatment did not lead to any deterioration in the properties of MFC and MFC/NaCMC blend, but an increase in the viscosity and in the storage and loss moduli was observed, probably because exposure of MFC to shear forces and high temperature under jet cooking further disintegrates or disperses MFC. The addition of NaCMC to a MFC suspension led to a relatively high viscosity of the MFC/NaCMC mix after jet cooking, due to a dispersing effect of NaCMC and because jet cooking gave a more efficient mixing of the materials.

Keywords: hydrothermal treatment, microfibrillated cellulose, MFC, carboxymethyl cellulose, NaCMC, hydrolysis, degradation, rheology

Foreword and acknowledgements

This thesis is based on studies that were carried out at Lappeenranta-Lahti University of Technology over the period of 2012-2019. This study has received funding from Stora Enso Oyj and the financial support is gratefully acknowledged. A grant from Research Foundation of Lappeenranta University of Technology is also greatly acknowledged.

I wish to express my gratitude to my supervisor, Docent Kaj Backfolk, for his encouragement, guidance and patience during this work. The reviewers of this manuscript are acknowledged; Professor Raimo Alén is thanked for his careful evaluation and suggestions for correction and Professor Ulf Germgård is thanked for his valuable comments and questions.

I am grateful to Lic. Tech. Isto Heiskanen from Stora Enso Oyj for co-operation and for the fruitful discussions over the years. I am also grateful to my co-authors, particularly D. Sc. (Tech.) Klaus Niemelä from VTT Technical Research Centre of Finland for his analytical efforts and discussions. Dr. Anthony Bristow is appreciated for the linguistic review of the papers and of this manuscript.

I would like to express my sincere thanks to the current and former staff of our research group. Especially Dr. Krista Koljonen, Teija Laukala (M.Sc.), Johanna Lyytikäinen (M.Sc.) and Dr. Katja Lyytikäinen are thanked for their help and for creating a pleasant working atmosphere.

Finally, I owe my family, relatives, and friends a debt of gratitude for their support.

Salla Hiltunen
August 2019
Lappeenranta, Finland

Contents

Abstract

Foreword and acknowledgements

Contents

List of publications	9
Abbreviations	11
1 Introduction	13
2 Objectives of the study	15
3 Cellulose-based thickeners	17
4 Hydrothermal stability	21
4.1 Hydrolysis of cellulose and hemicelluloses	21
4.2 Hornification and structural changes of fibers	24
4.3 Formation of chromophores	25
4.4 Hydrothermal stability of MFC	26
4.5 Hydrothermal stability of NaCMC	28
5 Materials and methods	31
5.1 Pulps	31
5.2 Enzymatic pretreatment	32
5.3 Mechanical fibrillation by fluidization	32
5.4 NaCMC grades	33
5.5 Hydrothermal batch experiments	34
5.6 Jet cooking	34
5.7 Rheological measurements	35
5.8 Water retention	35
5.8.1 ÅA-GWR	35
5.8.2 Centrifugal method	35
5.9 UV/VIS, color and brightness	36
5.10 XPS	37
5.11 Analysis of filtrates	37
5.12 Surface charge	39
6 Results and discussion	41
6.1 Effect of hydrothermal treatment on properties of MFC	41
6.1.1 Viscosity	41
6.1.2 Oscillatory measurements	43

6.1.3	Water retention	44
6.1.4	Surface charge	47
6.1.5	Discoloration	49
6.1.6	Hydrolysis products	51
6.1.7	Effect of pH on rheological properties of non-hydrothermally-treated samples	55
6.2	Hydrothermal stability of NaCMC	56
6.2.1	Viscosity	56
6.2.2	Discoloration	57
6.2.3	Surface charge	58
6.2.4	Hydrolysis products	59
6.3	Short-term steam treatment of NaCMC and MFC	61
6.3.1	Rheological properties	61
6.3.2	Short-term steam-treatment tests with MFC/NaCMC Mix	62
7	Conclusions	65
	References	67
	Publications	

List of publications

I

Hiltunen, S., Chunlin, C., Willför, S. & Backfolk, K. (2018). Thermally induced degradation of NaCMC in water and effects of NaHCO_3 on acid formation and charge *Food Hydrocolloids*, 74C, pp. 32-36.

II

Hiltunen, S., Heiskanen, I. & Backfolk, K. (2018). Effect of hydrothermal treatment of microfibrillated cellulose on rheological properties and formation of hydrolysis products *Cellulose*, 25(8), pp. 4653-4662.

III

Hiltunen, S., Heiskanen, I. & Backfolk, K. (2019). Short-term steam treatment of MFC gel with and without water-soluble cellulose derivative *Nordic Pulp & Paper Research Journal*, 34(1), pp. 10-18.

IV

Hiltunen, S., Koljonen, K., Niemelä, K., Heiskanen, I., Johansson, L.-S. & Backfolk, K. Hydrothermally induced changes in properties of MFC and characterization of the low-molar mass degradation products. *Cellulose*. Accepted.

Author's contribution in the listed publications

I The author planned and carried out all experiments excluding the determination of the molecular weight distributions. The results were interpreted and the manuscript written together with the co-authors.

II The author planned and carried out all experiments and analyses. The paper was written together with the co-authors.

III The author planned the experiments and participated in the experimental work, excluding the BET, XRD and SEM -measurements. The results were interpreted and the manuscript was written together with the co-authors.

IV The author planned and carried out the experiments excluding the analysis of filtrates, polyelectrolyte titrations, XPS measurements and microscoping. The results were interpreted and the manuscript was written together with the co-authors.

Supporting articles

Hiltunen, S., Sirén, H., Heiskanen, I. & Backfolk K. (2016). Capillary electrophoretic profiling of wood-based oligosaccharides, *Cellulose*, 23(5), 3331-3340.

Hiltunen, S. & Sirén, H. (2013). Analysis of monosaccharides and oligosaccharides in the pulp and paper industry by use of capillary zone electrophoresis: a review, *Analytical and Bioanalytical Chemistry*, 405(17), 5773-5784.

Abbreviations

DS	degree of substitution
ECF	elemental-chlorine-free
ECU	endo cellulase units
G'	storage modulus
G''	loss modulus
GC/MS	gas chromatography/mass spectrometry
5-HMF	5-hydroxymethylfurfural
HPLC	high performance liquid chromatography
M	molar mass
MCC	microcrystalline cellulose
MFC	microfibrillated cellulose
NaCMC	sodium carboxymethyl cellulose
NFC	nanofibrillated cellulose
PDADMAC	polydiallyldimethylammonium chloride
°SR	Schopper-Riegler
TEMPO	2,2,6,6-tetramethylpiperidinyloxy
UV	ultraviolet light
VIS	visible light
WRV	water retention value
XPS	X-ray photoelectron spectroscopy
ÅA-GWR	Åbo Academi gravimetric water retention

1 Introduction

Cellulosic nanomaterials such as microfibrillated cellulose (MFC) and nanofibrillated cellulose (NFC) are emerging materials that are produced from lignocellulosics by disintegrating fibers into smaller dimensions. Kraft pulp fibers typically have a fiber length of some millimeters and a width of tens of micrometers, but microfibrillated celluloses typically have a length on a micrometer scale and a width less than 100 nm (Kibblewhite & Hamilton 1984, Siro & Plackett 2010, Lavoine et al. 2012, Khalil et al. 2014, Klemm et al. 2018).

Fibrillation of wood fibers into fibrils using mechanical devices is an energy-intensive process and several pretreatment methods have therefore been developed, including both biochemical and chemical treatments as shown in Table 1.1. The MFCs prepared with various pretreatment methods differ from each other in their morphology and surface properties (Naderi & Lindström 2016). Microfibrillated celluloses prepared by a chemical pretreatment usually have a higher charge and a narrower size distribution than those prepared by enzymatic pretreatment (Naderi & Lindström 2016).

Table 1.1: Microfibrillated celluloses prepared using various pretreatment methods (Siro & Plackett 2010, Nechyporchuk et al. 2016).

Pretreatment method	Functional groups	Charge
Enzymatic	OH, COOH	anionic
TEMPO oxidation	CHO, COOH, OH	anionic
Carboxymethylation	CH ₂ COOH, OH	anionic
Quaternization	CH ₂ CHOHCH ₂ N(CH ₃) ₃ Cl	cationic
Sulfonation	SO ₃ H, OH	anionic
Phosphorylation	PO ₃ H ₂ , OH	anionic

The end product is a fibrillous cellulose gel with very high surface area, high viscosity, and high water retention capacity (Herric et al. 1983). The new properties and chemical functionality of MFC mean that they have a vast application potential in many fields (Cowie et al. 2014, Shatkin et al. 2014, Lindström et al. 2015). In paper and packaging applications, MFC can be used as an additive to increase the relative bonded area and improve the strength properties which also makes possible a source reduction (Shatkin et al. 2014, Lindström et al. 2015). The high strength is also beneficial in construction and composite preparation, where MFC may be used as reinforcement additive. The film-forming ability and good oxygen barrier properties are promising in barrier applications

and make MFC an interesting candidate to replace plastics in some applications (Wang et al. 2018). The rheology-modifying properties may be beneficial in the food, cosmetic, oil, and paint industries (Herric et al. 1983, Cowie et al. 2014, Shatkin et al. 2014, Lindström et al. 2015).

MFC may be exposed to hydrothermal treatment at temperatures above 100 °C depending on the operating or processing conditions and some applications therefore require more attention to the hydrothermal stability. The conditions depend largely on the application, and the treatment time at a high temperature may vary from seconds or minutes (heat sterilization, cooking) up to days or weeks (oil industry) and the temperature levels are typically between 100 and 200 °C. In the food industry, MFC has a potential to be applied as viscosifier, stabilizing agent for emulsions, and for its good water-retention properties. It is important that some of the physical properties are maintained although cooked, baked or fried. The processing at high temperatures should not lead to any harmful degradation by-products. In the oil industry, MFC is gaining interest to replace synthetic polymers for environmental reasons. MFC can be used in drilling, hydraulic fracturing, and in flooding agents due to its viscosifying properties, and MFC should therefore withstand the temperatures in oil wells (Lindström et al. 2015, Heggset et al. 2017). In some applications, such as in the pharmaceutical or cosmetic industries, safety and purity may require thermal sterilization.

Many of the thermal stability tests on MFC have been carried out in the dry state (Johnson et al. 2009, Eyholzer et al. 2010, Quivy et al. 2010, Tingaut et al. 2010) or where the temperature in the hydrothermal treatment has been below 100 °C (Herric et al. 1983, Iotti et al. 2011, Naderi & Lindström 2016). Only a few studies (Heggset et al. 2017) have measured the effects of high temperature on the properties of wet MFC and there is therefore still a lack of understanding of the effects of hydrothermal treatment at high temperatures (above 100 °C) on the properties of cellulosic nanomaterials.

2 Objectives of the study

The aim of the work described in this thesis has been to study how hydrothermal exposure influences the physicochemical properties of MFCs and to determine the conditions required to obtain a break-down of MFC gels. The MFC gels were prepared from enzymatically pretreated pulps. NaCMC was used as a comparative system because NaCMC and MFC partly overlap with their functionality as both have viscosity increasing and water-retaining properties and they are prepared from renewable sources. Changes in certain properties, viscosity, viscoelastic behavior and water retention capacity, were measured. In addition, the effects of hydrothermal treatment on the charge and discoloration were measured. The formation of low molar mass degradation products was evaluated in order to obtain further information about the hydrolysis reactions occurring and the chemical changes in MFC structure. An experiment was also carried out with model compounds (xylose and glucose) to determine whether the degradation products come from xylan or cellulose or both.

3 Cellulose-based thickeners

Cellulose-based thickeners are cellulosic particles or polymers that are used in various applications to increase the stiffness and viscosity, to modify the rheological properties and to prevent the phase separation or flocculation of particles (Clasen & Kulicke 2001). Thickeners may be prepared from purified and partially depolymerized cellulose, such as microcrystalline cellulose (MCC), or the chemistry of cellulose polymers can be modified to achieve more value leading to cellulose derivatives, mainly cellulose ethers (Thielking & Schmidt 2006, Trache et al. 2016, Nsor-Atindana et al. 2017). Cellulose ethers are prepared from alkali cellulose using various reagents (Alén 2011) and the properties of the cellulose ethers may be varied by the constituent type used, the degree of substitution and its uniformity. The molecular mass distribution of the cellulose chain also greatly affects the final properties (Clasen & Kulicke 2001, Thielking & Schmidt 2006, Alén 2011). During the preparation of a cellulose ether, side reactions occur, and cellulose ethers are therefore usually available either as a technical or as a purified grade.

Typical examples of cellulose ethers are methyl cellulose, ethyl cellulose, carboxymethyl cellulose, hydroxyethyl cellulose, hydroxypropyl cellulose, and ethyl(hydroxyethyl) cellulose (Clasen & Kulicke 2001, Thielking & Schmidt 2006, Alén 2011). Due to their solubility in water and good water-retaining capacity, cellulose ethers are used in several industrial areas including food, personal hygiene, and pharmaceutical products, oils, paints and coatings (Clasen & Kulicke 2001, Thielking & Schmidt 2006, Alén 2011). In addition to their viscosifying and rheology-modifying properties, they are also used for other purposes, such as moisture retention, preventing ice crystal formation, and improving oral feel and texture. Cellulose-based thickeners have high quality requirements, as they should be able to work in a variety of chemical and physical conditions such as pH, the frozen state or elevated temperature, and high salt concentration. Nor should they lead to any deterioration in the product properties such as clarity, taste, color or odor.

Sodium carboxymethyl cellulose (NaCMC) is commercially the most important cellulose ether and it has been used industrially for decades (Thielking & Schmidt 2006, Alén 2011). NaCMC has many beneficial properties. It is non-toxic, and it has remarkable solution-thickening and viscosity-modifying effects, good water-retaining capacity, and stabilizing effects. Many of these properties are also obtainable at low NaCMC solids content, e.g. <1 wt%, enabling cost-effective usage, especially with regard to high

viscosity grades. Theoretically the degree of substitution (DS) may vary between 0 and 3, but commercial grades are prepared with DS 0.5-1.5 (deButts et al. 1957). NaCMC grades with DS 0.4-1.4 have good solubility (Alén 2011) in both hot and cold water which makes NaCMC easy to use and also separates NaCMC from other cellulose derivatives that have a limited solubility in water, especially at elevated temperatures (Thielking & Schmidt 2006, Wüstenberg 2015). NaCMC solutions are, however, sensitive to changes in temperature and salinity (Abdelrahim et al. 1994, Gómez-Díaz & Navaza 2003, Yang & Zhu 2007, Khaled & Abdelbaki 2012). Monovalent salts cause coiling of the NaCMC polymer which decreases the viscosity, and multivalent salts reduce the solubility of NaCMC in water (Clasen & Kulicke 2001, Khaled & Abdelbaki 2012).

MFC and NFC offer a new choice as a rheology- or viscosity-modifying component and it is therefore important to clarify whether MFC can lead to any advantages or superior properties than the existing ones. MFCs are known to form a gel at very low concentrations in water, starting from 0.1-0.25 wt% (Pääkkö et al. 2007, Agoda-Tandjawa et al. 2010). Naderi & Lindström (2016) observed that MFC prepared from enzymatically pretreated pulp had a good stability against different salt concentrations (0-10 mM NaCl) whereas Lowys et al. (2001) and Agoda-Tandjawa et al. (2010) reported that added sodium chloride may even increase the gel-like behavior compared to that in salt-free conditions when MFC prepared from sugar-beet pulp is used. Instead, 2,2,6,6-tetramethylpiperidinyloxy (TEMPO)-oxidized and carboxymethylated microfibrillated celluloses have been shown to be rather sensitive to salinity (Jowkarderis & van de Ven 2014, Naderi & Lindström 2016) and the viscosity and gel properties decrease with increasing salt concentration. The temperature stability of nanocelluloses varies between different grades, but carboxymethylated MFC has been shown to have a good temperature stability at temperatures of 5-50 °C (Naderi & Lindström 2016). Table 3.1 compares some of the basic properties of MFC and NaCMC.

Table 3.1: Comparison of properties of MFC and NaCMC.

Property	MFC	NaCMC
charge	slightly anionic or anionic depending on chemical modification ¹	anionic and highly charged ²
crystallinity	40-60 % ³	low, affected by degree of substitution ⁴
hemicellulose content	depends on raw material prepared, 4-30 % ⁵	usually low ⁶
raw material	wood pulp, agricultural by-products ⁷	cotton linters, wood pulp ⁸
size	diameter < 100 nm, length in micrometer scale ⁹	radius of gyration < 200 nm ¹⁰
viscosity	highly shear thinning ¹¹	shear thinning or near Newtonian ¹²
water solubility	non-soluble ¹³	good solubility at DS 0.4-1.4 ¹⁴
appearance in water	whitish or transparent gel ¹⁵	transparent or yellowish liquid or gel ¹⁶

¹ Nechyporchuk et al. (2016), Naderi et al. (2016) ² Thielking & Schmidt (2006)

³ Iwamoto et al. (2007), Siró et al. (2011) ⁴ Lopez et al. (2015)

⁵ Arola et al. (2013), Naderi et al. (2016) ⁶ Lorand (1939)

⁷ Siro & Plackett (2010), Lavoine et al. (2012) ⁸ Stigsson et al. (2005), Lorand (1939)

⁹ Siro & Plackett (2010) ¹⁰ Gondo et al. (2006), Chatterjee & Das (2013) ¹¹ Heric et al. (1983), Pääkkö et al. (2007), Naderi et al. (2016)

¹² Ghannam & Esmail (1997), Thielking & Schmidt (2006), Benchabane & Bekkour (2008) ¹³ Wüstenberg (2015) ¹⁴ Alén (2011)

¹⁵ Nechyporchuk et al. (2016) ¹⁶ Wüstenberg (2015)

4 Hydrothermal stability

Hydrothermal treatment is the treatment of lignocellulosic biomass in water at an elevated temperature and pressure. It is typically carried out at temperatures between 150 and 250 °C and is also known as autohydrolysis, hot-water treatment, pressurized liquid water extraction or hydrothermolysis (Garrote et al. 1999, Gullón et al. 2012, Borrega & Sixta 2015). The hydrothermal treatment of cellulosic materials has been previously studied and is applied on an industrial scale as a prehydrolysis step prior to kraft pulping in the production of dissolving pulps (Conner 1984) that have a high cellulose content (>90 wt%) and low amounts of hemicelluloses and lignin (Borrega et al. 2017). Dissolving pulps are used in the manufacture of cellulose derivatives and regenerated cellulose (Borrega et al. 2017). The exposure of cellulosic materials to a thermal treatment in the aqueous state is also of interest in the hot-water hydrolysis used for the partial isolation of hemicelluloses from lignocellulose either as a pre- or as a posttreatment (Helmerius et al. 2010, Song et al. 2012, Borrega et al. 2013).

In the case of MFC and NaCMC, the hydrothermal stability describes the ability of the material to remain in its original state and to maintain functionality and partly defines its suitability for different applications. Hydrothermal treatment can affect the properties on a macroscopic and on a molecular scale. On a macroscopic scale, the hydrothermally induced changes are related to entanglement, flocculation or association of the fibrils. On a molecular scale, hydrothermal treatment may induce depolymerization and hydrolysis reactions that affect the chemical composition, surface properties or material dimensions. Molecular-scale changes also have an effect on the short-distance interactions between the fibrils.

4.1 Hydrolysis of cellulose and hemicelluloses

Cellulose has a relatively high resistance to hydrothermal treatment due to its semi-crystalline structure, linearity and high molecular mass (Borrega et al. 2011). Cellulose degradation is thought to be faster in the amorphous areas in which the chains are more disordered and where the penetration of water is faster (Gehlen 2010). The autodissociation of water is enhanced at elevated temperatures leading to the formation of H^+ and HO^- ions. The reaction mechanism depends on the catalyzing agent (Bobleter 1994). Hydronium ions attack and break the glycosidic bonds whereas hydroxide ions attack the anomeric carbon (Bobleter 1994) (Figure 4.1). It has also been suggested

that water itself may cause breakage of cellulose chain. In general, the reaction pathway of hydrothermal treatment is close to acid hydrolysis, but there are also specific reactions occurring during hydrothermal treatment (Bobleter 1994, Garrote et al. 1999, Borrega et al. 2011). The hydrolysis reactions cause the long polymer chains to be first hydrolysed to oligosaccharides and monosaccharides and then further degraded into different degradation products such as acids and furans.

Furan compounds are formed in acid catalyzed dehydration reactions where water is liberated from glucose leading to the formation of 5-hydroxymethylfurfural (5-HMF). Several reaction pathways have been suggested in the literature for the formation of 5-HMF, both from cyclic and open chains from glucose (Theander & Nelson 1988, Rasmussen et al. 2014). 5-HMF may also further react, degrading to levulinic acid and formic acid or undergoing condensation or resinification reactions. 5-HMF may also rearrange to 1,2,4-benzenetriol, or react with glucose or other degradation products to form humins, which give a dark color to the hydrolyzates (Luijckx et al. 1991, Rasmussen et al. 2014)

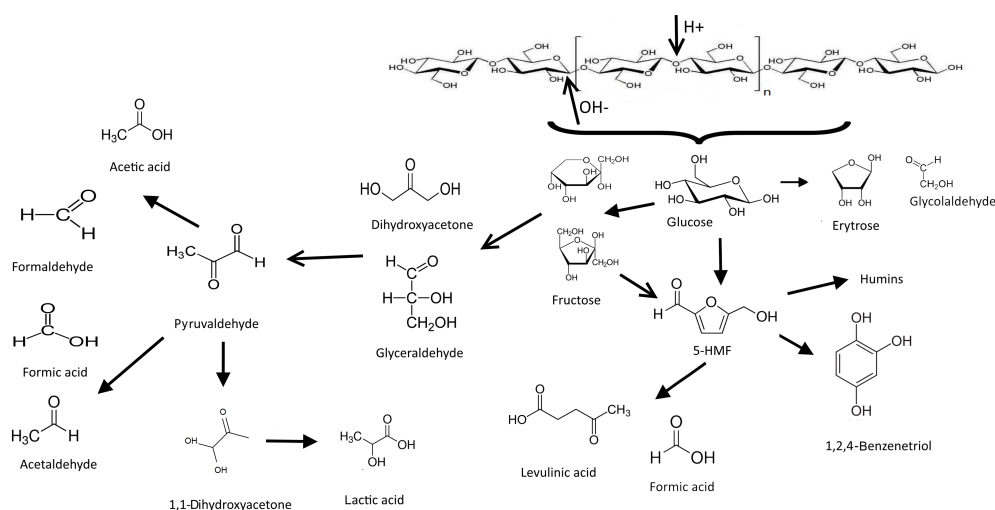


Figure 4.1: A possible reaction scheme for the formation of hydrolysis products from glucose. Modified from Bobleter (1994) and Cao et al. (2015).

High temperature and pressure may also initiate the isomerization or epimerization of monosaccharides, which means that glucose may convert to fructose or mannose, respectively. Isomerization is typically related to alkaline conditions, but relatively recent studies have found that it also occurs after severe ($T=180-350\text{ }^{\circ}\text{C}$) hydrothermal

treatment (Srokol et al. 2004, Aida et al. 2010, Lü & Shaka 2012, Borrega et al. 2013, Rasmussen et al. 2014). The isomerization process fastens the dehydration reactions, because the ring structure of fructose is less stable than that of glucose, and fructose is more often in its open-chain form.

The hydrothermal treatment of cellulosic materials have also been reported to produce various organic acids and some of them are the same as has been observed under alkaline conditions. Formic acid may be formed due to the rehydration of 5-HMF, but it has also been suggested that it can be formed from anomeric carbon. Glycolic, lactic and pyruvic acids have been identified as degradation products of cellulose in many studies (Niemelä & Sjöström 1986, Niemelä 1990, Yoshida et al. 2005). Part of the organic acid formation may possibly be through retrol-aldol condensation of saccharides into reaction intermediates i.e. glycolaldehyde, glyceraldehyde and dihydroxyacetone and their further degradation into organic acids (Srokol et al. 2004, Aida et al. 2010). Deoxyhexonic acids may also be formed from glucose or fructose through enediol formation and benzilic acid rearrangement (Luijkx et al. 1995).

Hemicelluloses have been found to be more reactive than cellulose due to their amorphous structure, side groups and branching and lower degree of polymerization (Conner 1984, Bobleter 1994, Alén 2015). It has been suggested that, during hydrothermal treatment, water autodissociation plays an important role at the beginning but that its importance diminishes as the reaction proceeds due to the formation of acidic degradation products (Garrote et al. 1999). In native hemicelluloses (xylans and galactoglucomannans), acetyl groups are cleaved and form acetic acid, facilitating the hydrolysis. In the case of kraft pulps most of the acetyl groups have been cleaved off during the cooking stages, and uronic acids have been converted to hexenuronic acids. Possibly hexenuronic acids also catalyze hydrolysis reactions. The hexenuronic acids may also be degraded to 2-furancarboxylic acid, 5-formyl-2-furancarboxylic acid and reductic acid (Sevastyanova et al. 2006b).

The hydrolysis of hemicellulose chains to oligo- and monosaccharides and then to various organic acids creates acidic conditions and lowers the pH in water. The hydrolysis of xylose has been reported to produce organic acids such as acetic, formic, lactic, glycolic and pyruvic acids (Oefner et al. 1992). These acids are partly the same as those that have been observed under alkaline conditions, but their quantity is smaller in plain water than under alkaline conditions (Oefner et al. 1992). The reactions possibly proceed in a similar manner to glucose with the isomerization of xylose to xylulose or epimerization

to lyxose. Relatively recent studies have shown that xylose is converted to xylulose at hydrothermal temperatures of 160-180 °C (Lü & Shaka 2012, Borrega et al. 2013). The reactions lead to the formation of trioses and pyruvaldehyde. The acids formed catalyze the formation of furfural from pentoses (xylose and arabinose). The reaction mechanism has been shown to be rather complex and both acyclic and cyclic reaction mechanisms for furfural formation have been suggested (Rasmussen et al. 2014).

4.2 Hornification and structural changes of fibers

The processing of cellulosic materials, such as thermal treatment, may cause structural reorganization (Weise 1998, Fahlén & Salmén 2003, Pönni et al. 2012, 2013). This reorganization is most often considered to be cellulose microfibril aggregation or the formation of irreversible bonds between cellulose microfibrils. Aggregation is often assumed to occur in the amorphous regime of cellulose. It has been suggested that hydrogen bonding can occur in the crystalline areas of cellulose as a cross-linking. Cross-linking may occur via lactone-bridge formation through hydroxyl and carboxyl groups and is promoted by heat and acidity (Potthast et al. 2010). The extent of structural reorganization depends on material characteristics and on process conditions, such as temperature, pH and moisture content (Pönni et al. 2012, 2013). Aggregation is strongly favoured during drying and dehydration and the hornification of dried samples has been recognized for a long time (Weise 1998, Kato & Cameron 1999, Diniz et al. 2004, Salmén & Stevanic 2018).

In the aqueous state, and especially in dilute systems, water between the fibril bundles hinders the aggregation. However, the coalescence of cellulose microfibrils have been observed during kraft pulping, linked to the removal of lignin and hemicelluloses (Fahlén & Salmén 2003). Acidic treatment at an elevated temperature may cause changes in the pulp that resemble those that occur during drying (Pönni et al. 2013). An increase in temperature also affects the properties of water and its solvent ability (Plaza & Turner 2015). Based on model calculations, it has been concluded that hydrothermal treatment may cause a hydration shell around cellulose to lose its structure and thus allow the aggregation of crystalline regimes in the of cellulose (cocrystallization) (Silveira et al. 2016). In a recent study (Ding et al. 2019) it was showed that hornification occurs during concentration of the nanofiber samples.

4.3 Formation of chromophores

Color is a quality parameter that affects the visual appearance and attractiveness of the product (Sandoval-Torres et al. 2010) and it is therefore important to consider the heat-initiated discoloration of cellulosic materials. However, it seems that the discoloration is a result of several reactions and is affected by the wood species and pulp type, the bleaching history, the content of oxidized groups and the content of hemicellulose and lignin as well as the presence of metal ions (Chirat & De La Chapelle 1999). The large number of chemical compounds contributing to the discoloration and, on the other hand, the very low concentration of the individual chromophores formed has hindered the identification of the chromophores (Rosenau et al. 2004).

It has been found that the discoloration is mainly related to reactions of hemicelluloses and lignin and that cellulose is more stable. Hexenuronic acids have been identified to be associated with thermal yellowing and, despite the acidic steps in bleaching, almost all bleached kraft pulps contain residual hexenuronic acids (Granström et al. 2001, Sevastyanova et al. 2006*b*). The hexenuronic acids are decomposed to 2-furancarboxylic acid, 5-formyl-2-furancarboxylic acids and reductive acids which may then further convert due to thermal or acidic stress to chromophoric structures (Sevastyanova et al. 2006*a*, Rosenau et al. 2017).

Chromophores are also formed by hydrolytic or oxidative reactions of hemicelluloses and cellulose at high temperatures and the formation of monosaccharides, oligosaccharides and acids which act as precursors for the discoloration process (Forsskåhl et al. 2000, Beyer et al. 2006, Korntner et al. 2015). Many of these color-forming substances or hydrolysis products are water-soluble and discoloration can be partly removed by rinsing with water. However, as the chemical reactions proceed, the discoloration becomes more resistant to water (Granström et al. 2001). The saccharides may further go through complicated redox and condensation reactions, leading to color-bearing compounds (Rosenau et al. 2004). These compounds may bond to the cellulose matrix, covalently or by adsorption.

In addition, carbonyl groups, keto- and carboxylic acid groups have been associated with discoloration (Chirat & De La Chapelle 1999, Lojewska et al. 2007). During hydrothermal treatment, the amount of carbonyl groups may increase due to depolymerization or oxidation reactions. In addition, chemical modification, such as TEMPO oxidation or carboxymethylation, creates highly oxidized groups on the cellulose

surface. During hydrothermal treatment, the discoloration of TEMPO-oxidized and carboxymethylated nanofibrillated celluloses has been found to be higher than that of chemically unmodified nanocelluloses (Heggset et al. 2017).

4.4 Hydrothermal stability of MFC

Heggset et al. (2017) studied the effects of hydrothermal treatment on nanocelluloses prepared with different pretreatment methods, and it was noticed that a three-day hydrothermal treatment at 110-150 °C led to molecular degradation of the gels, which was observed as a decrease in pH and the formation of furfural and 5-HMF. The highest temperature caused the greatest change in pH, indicating the greatest degradation. Nanocelluloses prepared with different pretreatment methods showed different stabilities against hydrothermal treatment. TEMPO-oxidized and carboxymethylated nanocelluloses showed poorer thermal stability than that of the chemically unmodified parent, based on the amount of furfural and 5-HMF after hydrothermal treatment. The addition of cesium or sodium formate improved the thermal stability of chemically unmodified nanocellulose and cellulose nanocrystals, probably because sodium formate acts as radical scavenger. It has been suggested that the thermo-oxidative depolymerization of cellulose probably plays a major role during hydrothermal treatment (Heggset et al. 2017).

Most of the experiments concerning the effect of temperature on the rheological properties of MFC have been carried out at temperatures below 100 °C. The temperature-dependence of viscosity seems to be partly affected by chemical modification. It has been reported that the viscosity of chemically unmodified MFC and NaCMC-grafted MFC suspensions decreases at temperatures of 5-80 °C (Herric et al. 1983, Iotti et al. 2011, Naderi & Lindström 2016), whereas carboxymethylated MFC has shown a high stability towards temperature in the 5-50 °C range (Naderi & Lindström 2016). At temperatures above 100 °C and a three-day treatment time, the viscosity of chemically unmodified nanocellulose has also been reported to decrease, but the decrease in viscosity was less than with xanthan and guar gums (Heggset et al. 2017).

The results of oscillatory measurements, are somewhat conflicting. Lowys et al. (2001) studied the effects of elevated temperature (25, 40 and 60 °C) on MFC prepared from sugar beet and noticed that neither the storage nor the loss moduli was affected by increasing the temperature. Lowys et al. (2001) pointed out that the high stability of the MFC suspension towards temperature differed from that of other polymers,

such as xanthan, which often show a decrease in rheological properties with increasing temperature. Similarly, in the case of MFC prepared from enzymatically pretreated pulp, Pääkkö et al. (2007) claimed that storage and loss moduli were not affected at temperatures below 40 °C and that a slight increase in the moduli was observed at higher temperatures (50-80 °C). The effect of temperature was similar at all studied gel concentrations (1, 2 and 5.9 wt%). On the other hand, Shafiei-Sabet et al. (2016) reported that the storage modulus decreased with increasing temperature (25-85 °C), causing a change from viscoelastic to liquid-like at 85 °C. The effect of temperature on storage modulus was more pronounced at a concentration of 2 wt% than at 1 wt%. According to Agoda-Tandjawa et al. (2010) and Shafiei-Sabet et al. (2016), MFC also showed thermoreversible properties, as the gel was able to recover its strength after heating and cooling the samples back to the initial conditions. Naderi & Lindström (2016) studied the effects of temperature (5-50 °C) on three different nanocellulose systems and reported that the storage and loss moduli decreased but that the decrease in loss modulus was higher, thus leading to increasing gel stiffness (G'/G'') in the case of MFC prepared from enzyme pretreated pulp. Carboxymethylated MFC showed good thermal resistance, as the storage and loss moduli were practically unaffected by temperature.

The ability of MFC to retain water is one of its key properties as it may form highly swollen gels even at very low concentrations in water, but the effects of hydrothermal treatment on the water retention of MFC are currently poorly known. Previous studies have reported that the fibrillation process increases the water-retention capacity (Herric et al. 1983, Iwamoto et al. 2005, Spence et al. 2010) as the solid structure of the fiber wall is broken and microfibrils are liberated leading to a high surface area (up to 200 m²/g). The amount of accessible hydroxyl groups which can form hydrogen bonds with water increases giving rise to swelling. Actually, it seems that the water-retention value of an MFC product can also be used as an indicator of the degree of fibrillation (Herric et al. 1983).

The interconnected web-like fibril structure means that a relatively large amount of water is bound between the fibrils and the rest of the water-retention capacity is affected by material properties (Maloney 2015). Microfibrillated celluloses prepared from raw materials containing large amounts of lignin (such as from thermomechanical pulp) have a poorer water retention than those prepared from chemical pulps and this is attributed to the hydrophobicity of chemically unmodified lignin (Spence et al. 2010, Lahtinen et al. 2014). Charge density is also an important factor affecting water retention (Saito

et al. 2007). In chemically unmodified MFC, the charge density is mainly related to the amount of hemicelluloses, especially residual hexenuronic and methylglucuronic acids. In addition, some residual lignin-bound carboxyls may occur. Pääkkönen et al. (2016) compared gravimetric water-retention values (ÅA-GWR) of TEMPO-oxidized nanofibrillated celluloses with their hemicellulose contents (0-25 %) and reported a significant decrease in water retention if the hemicellulose content was less than 10 %. Chemical modification such as carboxymethylation, cationization or surface grafting with polymers can be used to create highly charged surfaces, and this can increase the swelling capacity (Saito et al. 2007). The charged groups on the fibril surface gather around counter-ions which may cause differences in concentrations of mobile ions in the external phase and the fibrillous material, leading to an osmotic swelling pressure. Therefore changes in pH, salt concentration and the types of salt all have an effect on the water retention. Maloney (2015) studied the influence of different counter-ions on the swelling of TEMPO-oxidized nanofibrillated celluloses and observed that the Na^+ -form resulted in the highest swelling whereas Ca^{2+} gave the lowest swelling.

4.5 Hydrothermal stability of NaCMC

It has been reported that hydrothermal treatments at temperatures above 100 °C cause permanent changes in solutions of NaCMC (Rao et al. 1981, Hercules Incorporated 1999, CP Kelco Oy 2006-2009). Rao et al. (1981) concluded that heat treatment seemed to decrease both the hydrodynamic volume and the intermolecular interaction of NaCMC due to a partial hydrolysis of NaCMC chains. However, the ether bonds in the side groups of carboxymethyl cellulose are very strong and are not easily cleaved by acids (Reese et al. 1950). Only hot concentric acids can degrade the side groups (Reese et al. 1950, Graham 1971). Acid hydrolysis of NaCMC has been shown to produce glucose and its carboxymethyl-substituted derivatives, and hemicellulose-residues of monomeric sugars and their carboxymethyl substituted derivatives have also been found (Niemelä & Sjöström 1988). After high-temperature hydrothermal treatment at 250 °C, Kröger et al. (2013) reported that furans (furfural and 5-HMF), pentenes and benzenes were formed after only a few minutes of hydrothermal treatment.

Temperature has been reported to have a significant effect on the rheological properties of NaCMC (Abdelrahim et al. 1994), although at temperatures below 100 °C, the viscosity of the NaCMC solutions shows thermoreversible properties (Hercules Incorporated 1999, CP Kelco Oy 2006-2009). Several studies have reported a decrease in viscosity at

elevated temperature (Abdelrahim et al. 1994, Gómez-Díaz & Navaza 2003, Cancela et al. 2005, Yang & Zhu 2007). Gómez-Díaz & Navaza (2003) reported that increasing the temperature from 25 to 40 °C caused the NaCMC solutions to show a more Newtonian behavior. Mathematical models are often proposed to describe the flow behavior of NaCMC and a power law model is often chosen. An increase in temperature has been reported to reduce the consistency coefficient and increase the flow behavior index of the power law model over a wide temperature range (Rao et al. 1981, Abdelrahim et al. 1994, Abdelrahim & Ramaswamy 1995, Gómez-Díaz & Navaza 2003). However, it should be noted that the concentration of the NaCMC solution affected the parameters more than the temperature (Abdelrahim et al. 1994, Abdelrahim & Ramaswamy 1995). Heat treatment at temperatures above 100 °C has been reported to cause an irreversible decrease in the viscosity of NaCMC solutions due to hydrolytic decomposition (Rao et al. 1981, Thomas 1982).

In addition to the rheology-modifying properties of NaCMC solutions, their water-retention capacity is of importance in many applications. The water-retention capacity is related to the swelling and dissolution of the NaCMC polymer and to the amount of hydrophilic carboxymethyl groups that enable dissolution of the polymer (Thielking & Schmidt 2006). The particle size distribution also greatly affects the solution properties of NaCMC, as polymers with a high molecular mass usually dissolve more slowly in water. Higher concentrations enhance the formation of a network structure which gives a highly viscous and water-retaining solution (Thielking & Schmidt 2006). Hydrothermal treatments at high temperatures have been found to cause a reduction in water retention of NaCMC solutions (Thomas 1982).

5 Materials and methods

Figure 5.1 shows a simplified diagram of the work. Industrial, never-dried hardwood pulps were used as raw material and they were pretreated enzymatically prior to mechanical fibrillation using microfluidization. The microfibrillated celluloses were then exposed to hydrothermal treatment at different temperatures for different reaction times. In papers I, II, and IV, the hydrothermal treatment was carried out in closed metal containers, referred to as batch experiments. In paper III, short-term steam treatment using a continuous jet cooker was applied. NaCMC was used for comparison.

Different characterization techniques were adopted to gain information about the changes in the microfibrillated cellulose induced by the hydrothermal treatment and the subsequent effects on the suspension properties, as illustrated in Figure 5.1.

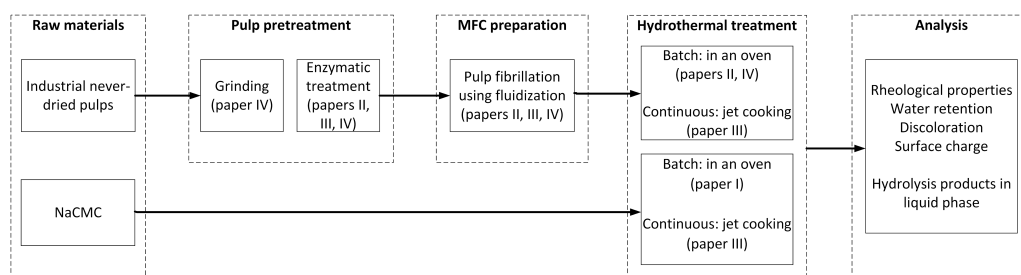


Figure 5.1: A diagram of the work.

5.1 Pulps

All the pulps used in this study were industrially produced and used in their never-dried state. The raw material of the pulps was hardwood.

Pulp 1 was a hardwood dissolving pulp (prehydrolysis kraft, Enocell, Stora Enso Oyj) that was elemental-chlorine-free (ECF) bleached containing approximately 5 wt% xylan (paper II). The pulp was received at 35 wt% consistency, and it was disintegrated according to SCAN-C18:65.

Pulp 2 was an elemental-chlorine-free (ECF) bleached birch kraft pulp (Stora Enso Oyj, Imatra) which was beaten to °SR 22 in a Voith LR 40 laboratory-scale refiner (specific

energy consumption ≈ 75 kWh/t) at a consistency of 4 wt%. The pulp contained approximately 25 wt% xylan (paper IV)

Pulp 3 was an ECF bleached, never-dried birch kraft pulp (Stora Enso, Imatra) containing approximately 25 wt% xylan (paper III).

5.2 Enzymatic pretreatment

All the pulps were enzymatically treated prior to mechanical fibrillation. The enzyme was a monocomponent endoglucanase (FiberCare R, Novozymes) with a declared activity reported by the supplier to be 4500 ECU/g, and this activity was used to calculate the dosage.

The enzymatic treatment process was adapted from Pääkkö et al. (2007) with slight modifications. Enzymatic treatments were carried out at 4 wt% pulp consistency, with an enzyme dosage of 2.2 mg/g_{pulp} (10 ECU/g_{pulp}) and the pH was adjusted to 7 using a phosphate buffer (11 mM KH₂PO₄ + 9 mM Na₂HPO₄). The enzymatic treatment was continued for 120 minutes for the pulp incubated at 45 °C on a water bath, the pulp suspension being mixed manually every 30 minutes. The enzymatic activity was terminated by boiling (95-100 °C) the pulp suspension for 30 minutes, followed by a washing step with deionized water (the conductivity of the pulp was adjusted with rinsing to 5 μ S/cm) in order to remove the buffer solution and enzyme protein from the sample.

5.3 Mechanical fibrillation by fluidization

MFC gels from different enzymatically pretreated pulps were prepared using a microfluidizer (M-110EH-30, Microfluidics Corp.). Two different chamber pairs connected in series were used, a large chamber pair with sizes of 400/200 μ m and a small chamber pair with sizes of 200/100 μ m. The pressures were 1100 bar for the larger chambers (400/200 μ m) and 1500 bar for the smaller chambers (200/100 μ m).

In the case of MFC A, the enzyme-treated Pulp 1 was diluted to a consistency of 2.0 wt% using deionized water. The pulp was run twice through the device using 400/200 μ m chambers and then three times using 200/100 μ m chambers (total 5 passes).

MFC B was prepared from beaten and enzyme-treated Pulp 2 diluted to a consistency of 2.0 wt%. The pulp was run twice through the device using two chambers connected in series with diameters of 400/200 μ mm and then three times using chambers connected

in series with diameters of 200/100 μm . Subsequent passes (=10) were all carried out with 200/100 μm chambers connected in series and a pressure of 1500 bar. The pulp was diluted every fifth time with deionized water (approx. 0.5 wt% units) in order to facilitate the feed in fluidization (total 15 passes) as shown in Figure 5.2.

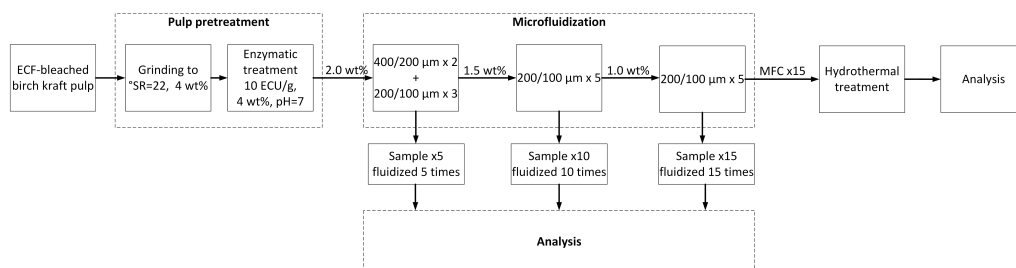


Figure 5.2: Preparation of the MFC B.

MFC C was prepared from Pulp 3. The enzyme-treated pulp was diluted with deionized water to a consistency of 3.0 wt% and was run twice through the device using the 400/200 μm chambers and then once using 200/100 μm chambers (total 3 passes).

5.4 NaCMC grades

Two different NaCMC grades were used. The NaCMC solutions were prepared from dried powders.

NaCMC I was a high viscosity grade obtained from Ashland (Blanose 7H5SCF). The average DS was 0.88, the purity 99.5 %, and the content of sodium glycolate was 0.4 % (reported by Ashland). NaCMC solution (1 wt%) was prepared by dispersing NaCMC in deionized water and then mixing overnight. The NaCMC solution was further diluted with deionized water to a concentration of 0.5 wt%.

NaCMC II was a low viscosity grade (FinnFix 30, CP Kelco, with minimum of 98 % NaCMC, DS=0.8 and M=80 000 g/mol). The dry NaCMC powder was gradually added to warm water (60 °C) under vigorous mixing with a Diaf-mixer until the solution was visually homogeneous. The mixing was then continued with a blade stirrer overnight at room temperature.

5.5 Hydrothermal batch experiments

Batch experiments (papers I, II, and IV) were carried out using metal containers (alloy C-276) having a volume of 200 mL. The containers were placed in an oven and the temperature and pressure were measured at the center of the container using a Pt100 - temperature sensor and pressure transmitter (PCE-28 Aplisens Ltd). After heat treatment, the samples were cooled in an ice bath (0 °C) to room temperature.

150 g of MFC A at a consistency of 2.0 wt% were placed in the containers and the samples were placed in an oven at target temperatures of 120, 150 and 180 °C. After introducing the samples, the oven regained the target temperature in 15 minutes. The samples were kept in the oven for 3, 10.5 and 24 hours. During the three-hour treatment, the samples had just reached the target temperature.

The containers were filled with 150 g of MFC B at 0.99 wt% consistency and placed in an oven at room temperature (20 °C). The oven was then heated to the reaction temperature of 150 °C during 11 minutes. The samples were kept in the oven for total times of 4, 6, 8, 12 and 24 hours. The samples reached the target temperature in 3 hours 30 minutes and the times at the temperature of 150 °C were thus 0.5, 2.5, 4.5, 8.5 and 20.5 hours. The pressure was approximately 4.5 bars.

The containers were filled with 140 g of 0.5 wt% NaCMC I solution and were placed in an oven at room temperature (23 °C). The oven was then heated to the reaction temperature (120, 140, 160 or 180 °C during approximately 30, 40, 50 and 60 minutes respectively). After the oven had reached the target temperature, the samples were kept in the oven for 2 hours.

5.6 Jet cooking

Thermal treatments of MFC C and NaCMC II were carried out using a pilot-scale steam jet cooker (Cerestar). The initial consistency of the samples was adjusted to approximately 1.5 wt% to reduce the viscosity of the gel and facilitate pumping and feeding into the jet cooker. The samples (30 L each) were then passed through a pilot-scale jet cooker at a low speed 3.0 ± 0.3 L/min. The temperature of the jet cooker was adjusted with hot steam to 130 °C and the pressure was approximately 3 bar. The samples were passed through the jet cooker 0-3 times and the introduction of steam diluted the samples in each cycle as shown in Table 5.1.

Table 5.1: Consistency of MFC (wt%) and dry solids content of NaCMC II (wt%) and of the MFC/NaCMC mixture during jet cooking (0-3 passes).

No. of passes	MFC [%]	pH	NaCMC [%]	pH	MFC/NaCMC 50/50 wt%	pH
0	1.42	7.4	1.34	7.6	1.35	7.4
1	1.01	7.8	1.02	7.7	1.02	8.0
2	0.81	7.9	0.88	7.6	0.83	8.3
3	0.64	8.0	0.76	7.6	0.67	8.4

5.7 Rheological measurements

A rheometer (Modular Compact MCR 302, Anton Paar) was used for the measurements. A concentric cylinder CC27 (MFC A, MFC B, MFC C and NaCMC II) or double gap DG 26.7 (NaCMC I) measuring geometries were used. Only smooth surfaces were employed. All measurements were carried out at 20 °C. The viscosities were measured with increasing shear rates of 0.1-1000 1/s. The linear viscoelastic domain was determined using an angular frequency of 10 rad/s (MFC A and MFC B) and 1 rad/s (MFC C). Frequency sweeps on MFC A and MFC B were performed at 100-0.1 rad/s using a strain of 0.1 %, and on MFC C at range 10-0.1 rad/s using a strain of 1 %.

5.8 Water retention

5.8.1 ÅA-GWR

The ability to dewater the MFC A (paper II) by membrane filtration was determined using a gravimetric and static water retention method (ÅA-GWR, DT Paper Science Oy), using a polycarbonate filter with 0.03 μm pore size, a pressure of 1 bar for 90 s, and a total contact time of 135 s. This method measures the amount of water released by the sample under given conditions, and a low value thus means that the water retention ability is high.

5.8.2 Centrifugal method

The water-holding capacity of the MFC B (paper IV) before and after hydrothermal treatment was determined using a centrifugal method described by Maloney (2015). Different quantities of MFC (0-13.6 wt%) were mixed with a matrix pulp based on ECF-bleached and ground hardwood pulp from which fines had been removed using a mesh of 200 (75 μm). The matrix pulp had been converted to its sodium form. The MFC and matrix pulp were mixed at 1 wt% total solids content for 30 minutes and the suspension

was then filtered on a filter paper using a Büchner funnel, and the filtrate was recirculated on the filter paper to ensure that all the MFC was captured in the matrix. During filtration, the solids content of the filtrate was maintained between 10 and 15 wt%, which was found to be crucial to obtain reproducible results. The filtered, wet pad (MFC+ pulp) was centrifuged for 15 minutes at 3100 g with constant acceleration and deceleration ramps. The dry grammage of the test pad during the centrifugation step was 1700 g/m² (pulp + MFC). After centrifugation, the samples were oven dried at 105 °C overnight, and the water-retention capacity was calculated as:

$$WRV_{total} = \frac{m_{wet} - m_{dry}}{m_{dry}}, \quad (5.1)$$

where

m_{wet} is the mass of the centrifuged wet test pad (gel + pulp), and
 m_{dry} is the mass of the oven-dry test pad = total mass of the sample

The hydrothermally induced aggregation of MFC was estimated by calculating the change in water retention:

$$Aggregation = \frac{WRV_0 - WRV_1}{WRV_0} \times 100, \quad (5.2)$$

where

WRV_0 is the water retention of the untreated MFC determined in a MFC/pulp mixture
 WRV_1 is the water retention after hydrothermal treatment of MFC determined in MFC/pulp mixture

5.9 UV/VIS, color and brightness

UV/VIS absorption spectra of the samples were obtained using quartz crystal cuvettes with a spectrophotometer (Jasco V-670). All measurements were made in triplicate.

UV/VIS absorption spectra of MFC B suspensions were obtained at wavelengths of 190-900 nm. Deionized water was used as a reference. The initial consistency of the gel in the hydrothermal treatment was 0.99 wt% and the heat-treated gels were measured without any rinsing.

Absorbance of NaCMC I was measured at wavelengths of 190-800 nm. The untreated sample (NaCMC in ion-exchanged water) was used as reference.

The colour and brightness of dried MFC B cakes were measured with a Lorentzen & Wettre Elrepho instrument. The MFC B cakes were prepared by vacuum filtration and the gels were rinsed with deionized water to remove water-soluble degradation products. Rinsing was continued until the electrical conductivity of the filtrate was close to that of the deionized water. The MFC cakes were then frozen and freeze-dried. The colour, brightness and yellowness of the cakes were measured with a blotter as a background, because the MFC cakes were not fully opaque. The values were calculated using D65/10° illuminant/observer conditions.

5.10 XPS

The MFC B samples for X-ray photoelectron spectroscopy (XPS) analysis were prepared by forming a fibril cake by vacuum filtration. During the filtration, the gels were rinsed with deionized water in order to remove water-soluble acids from the heat-treated gels, so that they would not give a signal during XPS analysis. The removal of the acids was monitored by measuring the electric conductivity of the filtrate. Before analysis, the fibril cakes were frozen at -18 °C and freeze-dried.

The surface compositions of the dry fibril cakes of MFC B were evaluated using the AXIS Ultra instrument (Kratos Analytical, U.K.). Samples were mounted on a sample holder using an ultra-high vacuum-compatible carbon tape and pre-evacuated overnight. A fresh piece of pure cellulosic filter paper (Whatman) was analyzed as an in-situ reference with each sample batch (Johansson & Campbell 2004). Measurements were made using monochromated Al K α irradiation at 100 W and under neutralization. Wide scans as well as high-resolution regions of C 1s and O 1s were recorded on several locations with a nominal analysis area of $400 \times 800 \mu\text{m}^2$. The analysis depth of the method is less than 5 nm. The data were analysed with CasaXPS, and binding energies in all spectra were charge-corrected using the main cellulosic C-O component at 286.7 eV as the reference (Beamson & Briggs 1992).

5.11 Analysis of filtrates

Filtrates of hydrothermally treated MFC B were prepared by centrifuging the gel samples (30 min, 4900 g) and filtering the supernatant once through a $0.45 \mu\text{m}$ PTFE syringe filter. It was difficult to separate water from the untreated sample by centrifugation and for this reason the non-heat-treated sample was first filtered through a cellulose fiber filter (12-15 μm) followed by through syringe filters of 5 μm and 0.45 μm .

In the experiments with model compounds, sugar solutions of 10 g/L were prepared using commercial grades of D-(+)-xylose (Sigma Aldrich $\geq 99\%$) and D-(+)-glucose (VWR, AnalaR Normapur).

Filtrates of MFC B were analysed for hydroxy carboxylic acids, sugars and other hydroxy compounds by gas chromatography mass spectrometry (GC/MS), for formic and acetic acids by capillary electrophoresis (CE) and for furfural and its 5-HMF by liquid chromatography (HPLC). The hydrothermally treated sugar solutions were analysed only by GC/MS. The sugar samples were also analysed for phenolic compounds. For GC/MS, 2 mL or 4 mL of MFC filtrates and 0.5 mL of xylose and glucose solutions were evaporated to dryness and trimethylsilylated (Borrega et al. 2013) prior to the analyses with a gas chromatograph equipped with a mass selective detector. For the separations of MFC filtrates, an RTX-5MS capillary column was used and for the separations of xylose and glucose a DB-5MS capillary column. The carrier gas was helium. The concentrations were calculated directly from the peak sizes, using xylitol as the internal standard.

For the analysis of the phenolic compounds in the hydrotreated sugar solutions, 5 mL liquor samples were extracted three times with 5 mL of diethyl ether, after the addition of salicylic acid as the internal standard. The ether phases were combined, evaporated to dryness, and analysed by GC/MS (after trimethylsilylation), as described for the unfractionated sugar solutions.

For the CE analyses, a P/ACE MDQ capillary electrophoresis (CE) instrument equipped with a photodiode array UV-VIS detector working by indirect detection at a wavelength of 230 nm (Beckman-Coulter Inc., Fullerton, USA) was used. Commercial electrolyte solutions from Analis (Ceofix Anions 5) were used. A bare fused silica capillary with an inner diameter of 75 μm was used, the detector length to the UV detector being 50 cm and the total length 60 cm. A separation voltage of 30 kV and polarity of positive to negative was applied. For the quantification of formic and acetic acids, corresponding standard solutions were prepared and analysed prior to the actual samples.

The furfural compounds in the filtrates of MFC B were quantified from the 0, 8.5 and 20.5 h samples using a HPLC-RI (Perkin Elmer, Flexar) system equipped with Aminex column (HPX-87H, Bio-RAD) under isocratic conditions (50 °C) at a flow rate of 0.5 mL/min of 2.5 mM H_2SO_4 . For the analysis of the phenolic compounds in the hydrothermally treated sugar solutions, 5 mL liquor samples were extracted three times with 5 mL of diethyl ether, after the addition of salicylic acid as the internal standard. The ether phases were

combined, evaporated to dryness, and analysed by GC/MS (after trimethylsilylation), as described for the unfractionated sugar solutions.

Free acid content of hydrothermally treated NaCMC I solutions was examined using high performance liquid chromatography (HPLC) with MetaCarb 87 H column and 5 mM H_2SO_4 as an eluent. The flow rate was 0.6 mL/min and the detection was at 210 nm. To determine the 5-HMF, the flow rate was increased to 0.8 mL/min (gradient elution) and detection was at 280 nm.

5.12 Surface charge

The charges of the materials were determined by polyelectrolyte titration using a streaming current detector (PCD 02, Müttek). The surface charge of MFC was calculated based on the cationic demand.

MFC A was directly titrated to the point of zero charge with 0.00025 N polydiallyldimethylammonium chloride (PDADMAC) solution ($M = 107\,000$ g/mol, BTG Instruments GmbH) and MFC A gel concentrations of 0.6-1.3 g/L. The pH of the samples was adjusted to $\text{pH} = 6.7 \pm 0.2$ with a titrator using 0.05 M NaOH solution, and the NaCl concentration during titration was approximately 0.5 mmol/L.

MFC B suspensions were titrated according to the method described by Junka et al. (2013). The gel was dispersed in deionized water at 1 g/L for 1 hour and then diluted to 0.5 g/L. The pH and ionic strength were adjusted using 0.1 M NaOH, 0.1 M HCl and 1 M NaHCO_3 . A known amount (10-30 mL: 0.1-0.5 g/L) of the MFC dispersion was titrated with PDADMAC solution ($M=400\text{-}500\,000$ g/mol, 0.25 or 1 meq/L, Sigma Aldrich Oy). The pH of the MFC dispersion was constantly measured and adjusted if necessary before titration.

NaCMC I solutions were titrated with 0.001 N PDADMAC and 0.001 N polybrene in deionized water. The pH of the samples was adjusted with 0.05 M NaOH solution to $\text{pH} = 6\text{-}7$.

6 Results and discussion

Hydrothermal treatment of MFCs prepared from enzymatically pretreated pulps has been carried out at different temperatures and for different times. Here, the effects of hydrothermal treatment on properties of MFC such as viscosity, viscoelastic properties and water retention are presented. The effect of hydrothermal treatment on the surface properties of MFC is discussed in relation to surface charge measurements made with polyelectrolyte titration. In addition, the effects of hydrothermal treatment on the discoloration of MFC are briefly discussed. The second part concentrates on the hydrolysis reactions occurring in the system and the analysis of filtrates. An experiment with model compounds (glucose and xylose) was carried out to study whether the degradation products originate in the cellulose, xylan or both. The results are compared with those for hydrothermally treated NaCMC to see whether there are great differences in the hydrothermal behavior of MFC and NaCMC. Co-addition of NaCMC to MFC was also studied, although the hydrothermal treatment conditions were different. They were selected to resemble an industrially scalable process and to see whether there were any synergistic effects.

6.1 Effect of hydrothermal treatment on properties of MFC

6.1.1 Viscosity

Figure 6.1a shows a viscosity curve of MFC A prepared in 0.01 M NaCl at a consistency of 2.0 wt% after exposure to hydrothermal treatment for different times at different temperatures. The untreated gel (Reference) had a strongly shear thinning viscosity with an intermediate transition area or kink in the viscosity curve. Heat treatment at 120-150 °C lead to no significant changes in the viscosity profile of the gels. The viscosity was almost constant even after hydrothermal treatment of 21 h at 120 °C or 150 °C for 7.5 h showing that MFC A had a good stability towards hydrothermal treatment, but when MFC A samples were heated to 180 °C, a lower viscosity was observed and the viscosity curve had a more irregular shape. The sample treated under the most severe conditions (180 °C, 21 h) had a much lower viscosity and a different shear rate-viscosity dependence. This temperature was found to be critical for the stability of the MFC gel.

Figure 6.1b shows the viscosity of MFC B prepared in ion-exchanged water at a consistency of 0.99 wt%, before and after hydrothermal treatment at 150 °C. Untreated MFC B (Reference) showed two shear thinning regions and a transition area between them

as previously observed for MFC A. When MFC B was exposed to hydrothermal treatment at 150 °C, the viscosity dropped already after the shortest treatment time (0.5 h) and the longest treatment time (20.5 h) resulted in the lowest viscosity value. The hydrothermal treatment also caused the intermediate transition area to shift to a higher shear rate, suggesting a change in the structure of the gel.

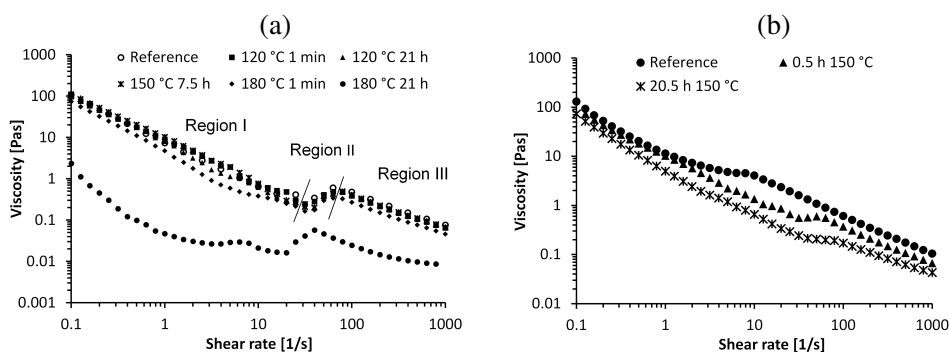


Figure 6.1: Viscosity of MFC A and MFC B measured at 20 °C as affected by the hydrothermal treatment. The flow behavior may be divided into 3 regimes. (a) MFC A prepared from dissolving pulp and exposed to hydrothermal treatment at a consistency of 2.0 wt%. (b) MFC B prepared hardwood kraft pulp and exposed to hydrothermal treatment at 0.99 wt%.

A type of shear-thinning viscosity similar to that of untreated MFC A and MFC B has previously been reported in many other studies of gels without any heat treatment (Pääkkö et al. 2007, Iotti et al. 2011, Naderi & Lindström 2016). The kink in the viscosity curve is assumed to occur due to a change in the floc structure of the gels (Karppinen et al. 2012, Saarikoski et al. 2012) leading a characteristic three-regime behavior with increasing shear rate as previously reported by Iotti et al. (2011) and by Naderi & Lindström (2016). Small shear rates are assumed to create conditions for a slow orientation and reorganization of the flocculated network structure and fibril alignment, and thus the decrease in viscosity is relatively linear (Region I). In the intermediate transition region, the viscosity increases and this is assumed to be due to a separation of the network structure into individual fibril flocs and fibril-free voids (Region II). In the third region at high shear rates, the fibrils and flocs move relative to each other and the floc size may decrease (Karppinen et al. 2012, Saarikoski et al. 2012).

A decrease in viscosity after hydrothermal treatment of different MFCs has previously been reported by Heggset et al. (2017), but the exposure time was much longer than in

the present study. The observed differences in ability of MFC A and MFC B to withstand hydrothermal treatment are assumed to be partly affected by the raw material composition, as MFC A was prepared from a hardwood dissolving pulp and MFC B from a hardwood kraft pulp. The dissolving and kraft pulps have different amounts of hemicelluloses and charges. Hemicelluloses with a more amorphous structure than cellulose are more affected by the hydrothermal treatment. Part of the difference may also be related to consistency, as with higher solids content the interfibrillar network dominates and a small heat-initiated degradation does not cause as remarkable a change in viscosity as it does at lower consistencies. The level of fibrillation or the fineness of the MFC gel may also play a part, as a larger surface area may increase the rate of degradation.

6.1.2 Oscillatory measurements

Figure 6.2a shows the storage (G') and loss modulus (G'') of MFC A before and after hydrothermal treatment. The storage modulus (G') dominated over the loss modulus (G'') at all data points, confirming a gel-like structure. The storage modulus was about ten times greater than the loss modulus (the loss factor $\tan \delta = (G''/G')$ being approximately 0.1) which is consistent with previous results with enzymatically pretreated MFC where loss factors less than 0.3 have been reported (Pääkkö et al. 2007, Naderi & Lindström 2016). The storage modulus of the untreated sample (≈ 700 Pa) was also approximately at the same level as previously reported for enzymatically pretreated MFC, measured at 2 wt% by Naderi & Lindström (2016). When MFC A in the present study was exposed to hydrothermal treatment at 120 °C for 21 h and 150 °C for 7.5 h, the storage and loss moduli of MFC A surprisingly increased slightly. At 180 °C or with the longest reaction time, the opposite behavior was observed and both moduli decreased.

Figure 6.2b shows storage and loss moduli of MFC B before and after hydrothermal treatment at 150 °C. MFC B had a storage modulus about six times higher than the loss modulus (loss factor ca. 0.17). Also in this case, both the moduli increased with treatment times of 0.5-8.5 h but decreased with the longest treatment time (20.5 h).

The observed increase in storage and loss moduli due to hydrothermal treatment indicates a stiffening of the gel network or an enhancement of fibril-fibril interactions. This may occur for several reasons, such as the dissolved components strengthening the gel or that the fibrils becoming more hydrophobic. The possibility of structural reorganization and microfibril aggregation induced by the hydrothermal treatment may also lead to stiffening of cellulose microfibrils (Pönni et al. 2013, Silveira et al. 2016). Hydrolysis

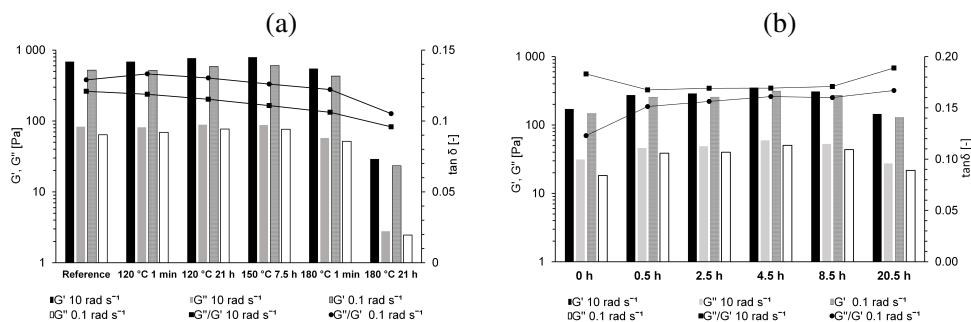


Figure 6.2: (a) Storage (G') and loss (G'') moduli and loss factor $\tan \delta = (G''/G')$ of MFC A as affected by conditions of thermal treatment. Measurements were performed at 0.1 % strain. (b) Storage (G') and loss (G'') moduli of MFC B as affected by hydrothermal treatment at 150 °C. The storage (G') and loss (G'') moduli of the gels measured at 20 °C and the strain used was 0.1 %.

of hemicelluloses and charges may induce higher gel strength because the electrostatic repulsion between the fibrils is reduced. Arola et al. (2013) reported that the removal of xylan from NFC surface by enzymatic hydrolysis increased the sample storage modulus if the sample was not mixed during the hydrolysis, showing that the removal of xylan may enhance the formation of a MFC network, but the history of processing affects the results. On the other hand, Pääkkönen et al. (2016) reported that removal of hemicelluloses by cold alkali extraction resulted in a weaker gel structure of TEMPO-oxidized NFC and a gel that was less elastic.

6.1.3 Water retention

Figure 6.3a shows the water-retention values of MFC B/pulp mixtures (paper IV) as a function of MFC content before and after hydrothermal treatment, measured using a centrifuge technique. Initially, the water retention capacity increased almost exponentially with increasing MFC loading and the samples were difficult to dewater, particularly with the highest MFC loadings (8.7 and 13.6 wt%). Hydrothermal treatment caused the water retention value to decrease and it was linearly dependent on the MFC loading. Figure 6.3b shows the effect of hydrothermal treatment time on the water-retention with MFC contents of 4.2 wt% and 13.6 wt%. The decrease in water retention was most pronounced at short reaction times (0.5-4.5 h), but it stabilized to a certain level with longer treatment times (8.5 and 20.5 h).

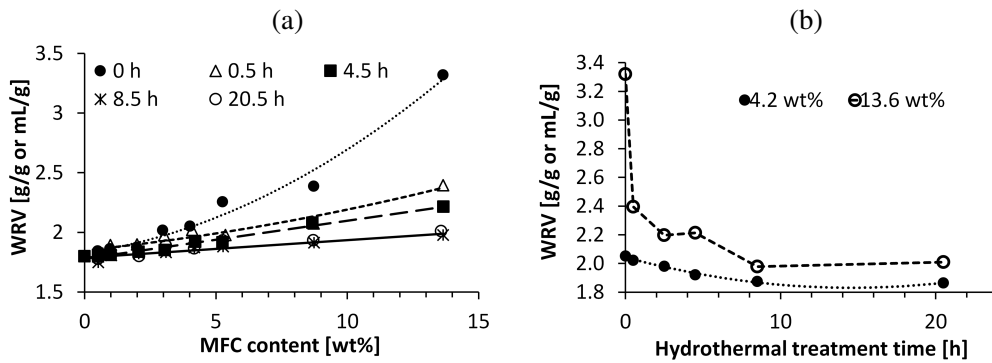


Figure 6.3: (a) Water retention value of MFC/pulp mixtures (paper IV). Effect of hydrothermal treatment on water retention after 0, 0.5, 4.5, 8.5 and 20.5 h treatments at 150 °C. (b) Effect of hydrothermal treatment time on water retention capacity with MFC contents of 4.2 wt% and 13.6 wt%.

In the case of MFC A (paper II), the water retention decreased after the hydrothermal treatment (Table 6.1). In this case, the water retention capacity was measured using the modified ÅA-GWR -method. An increase in the amount of water released and thus a decrease in the water retention ability of the gels was observed already after a short hydrothermal treatment (120 °C 1 minute), and was at roughly the same level for the samples treated at 120 °C 21h, 150 °C 7.5 h and 180 °C 1 minute. The microfibrillated cellulose gel treated at the highest temperature (180 °C) for 21 h showed a significant drop in the water retention value.

Table 6.1: Released water (modified ÅA-GWR) and pH of MFC A after hydrothermal treatment.

Sample	ÅA-GWR [g/m ²]	pH
Reference	595	6.4
120 °C 1 min	790	5.9
120 °C 21 h	1186	4.6
150 °C 7.5 h	1055	4.1
180 °C 1 min	1142	3.9
180 °C 21 h	1575	3.1

In fibrillated material, a large amount of water is held between the fibrils that form an interconnected network structure. The rest is intraparticle water that is affected by the material properties such as pore size distribution, pore volume and amount of charged groups (Maloney 2015). There are several possible explanations for the observed loss of water retention ability after hydrothermal treatment. The treatment may cause the hydrolysis of hemicelluloses and charged groups, where the hydrolysis products are released into solution so that they no longer act as part of the fibrils and thus do not contribute to gel swelling. The heat treatment reduces the pH of the gels (Table 6.1) due to acid formation and this means that the charged groups are partly protonated, reducing the gel swelling. It is also possible that long-term heat treatment degrades the amorphous areas of cellulose which are typically more swollen than the crystalline parts. Aggregation of fibrils reducing the surface area may also occur during hydrothermal treatment. Previously, water retention has been used as a measurement technique to estimate the extent of cellulose microfibril aggregation, although it is a relatively rough method (Weise 1998, Welf et al. 2005, Pönni et al. 2013). A decrease in WRV as a consequence of microfibril aggregation has been observed (Welf et al. 2005, Pönni et al. 2013) and Pönni et al. (2013) reported that the aggregation of cellulose microfibrils in the wet state may occur already at temperatures below 100 °C.

Using MFC B as an example and neglecting all other possible effects on water retention, the decrease in water retention capacity due to aggregation was estimated using MFC/pulp mixtures with MFC loadings of 4.2 and 8.7 wt% (Table 6.2). Hydrothermally induced "aggregation" was calculated according to equation 5.2 and it was found that aggregation was strongly dependent on MFC loading, as previously observed with water retention values of MFC/pulp mixtures. With MFC loading of 4.2 % the "aggregation" was less than 10 % but with MFC loading of 8.7 wt% it was much higher, up to 20 % after the longest treatment times at 150 °C. Previously, Pönni et al. (2013) reported that hydrothermal treatment of pulp under acidic conditions resulted in an approximately 5 % decrease in water retention whereas drying has been reported to cause a much greater decrease in water retention, up to 30-50 % (Welf et al. 2005, Kontturi & Vuorinen 2009)

Table 6.2: Estimated aggregation [%] of MFC B/pulp mixtures after hydrothermal treatments of MFC at 0-20.5 h at 150 °C. Calculated as the change in WRV.

Hydrothermal treatment time [h]	Aggregation [%]	
	MFC content [wt%]	
	4.2	8.7
0		
0.5	1.5	13.1
2.5	3.5	12.7
4.5	6.4	12.9
8.5	8.6	19.9
20.5	9.1	19.0

6.1.4 Surface charge

Polyelectrolyte adsorption was used in the determination of surface charges of MFC grades before and after hydrothermal treatment. Table 6.3 shows that MFC A initially had a low amount of surface charges, 20 $\mu\text{eq/g}$, which was expected since MFC A was made from dissolving pulp having a low content of hemicelluloses, and essentially no lignin or resin. The surface charge remained practically constant after hydrothermal treatment treatment at 120-150 °C. Only after a long treatment time (21 h) at 180 °C did the surface charge notably increase. The surface charge of untreated MFC B was 53 $\mu\text{eq/g}$,

Table 6.3: Surface charge of MFC A or MFC B. The pH of the MFC A samples was adjusted to 6.7 ± 0.2 before the surface charge was measured. Surface charge of MFC B (fluidized 15 times) was measured at pH 8.5 using 0.01 mM NaHCO_3 buffer.

MFC A	$\mu\text{eq/g}$	MFC B	$\mu\text{eq/g}$
Reference	21	Reference	53
120 °C 1 min	22	150 °C 0.5 h	17
120 °C 21 h	23	150 °C 2.5 h	15
150 °C 7.5 h	27	150 °C 4.5 h	13
180 °C 1 min	20	150 °C 8.5 h	13
180 °C 21 h	129	150 °C 20.5 h	14

which is higher than that of MFC A because MFC B was prepared from hardwood kraft

pulp. Hydrothermal treatment caused the surface charge of MFC B to decrease drastically already after the first 0.5 hours of treatment time at 150 °C. When the treatment time was increased to 2.5-20.5 hours, there was no further effect on the surface charge.

As the MFC grades used in this study were prepared from bleached hardwood kraft pulp or bleached prehydrolysis kraft hardwood dissolving pulps, it is assumed that hexenuronic acids and residual 4-*O*-methylglucuronic acids were the main factors affecting the charge carried by the MFC (Sjöström 1989, Teleman et al. 1995, Vuorinen et al. 1996). The effects of carboxyl or phenolic hydroxyl groups in lignin and of uronic acids from pectins are assumed to be negligible. However, it was assumed that, as the degree of fibrillation or fineness of the MFC increased, the surface charge approached the total charge which is determined by conductometric or potentiometric titration. It was also assumed that the total charge was not affected by the microfluidization process (Pääkkö et al. 2007). Previously, for ECF-bleached birch kraft pulps with a low lignin content (kappa number < 3), it has been reported that the total charge of pulp was 45-90 $\mu\text{eq/g}$ measured in a pH range of 7.5 to 8 (Laine & Stenius 1997, Lyytikäinen et al. 2011). For dissolving pulps, a total charge ranging from 20 to 30 $\mu\text{eq/g}$ has previously been reported under near neutral conditions (Notley 2008, Olszewska et al. 2011, Naderi et al. 2016).

The decrease in surface charge of MFC B due to hydrothermal treatment may occur because the hexenuronic acid groups are destroyed by the high temperature, by the low pH and long treatment times. Vuorinen et al. (2004) reported that it is possible, by treating cellulosic suspensions in water at temperatures above 90 °C and at pH of 2-5 for about 10 minutes, to selectively remove hexenuronic acids from pulp. However, this does not explain what residual charges were not affected when the hydrothermal treatment time was extended or why with MFC A the surface charge remained practically constant at temperatures of 120-150 °C. It is possible that the residual charges are related to oxidised cellulose structures that are formed during the bleaching process or that new ones are created by the hydrothermal treatment. A clear difference in the surface charge of MFC was observed after hydrothermal treatment at the highest applied temperature (180 °C) and the longest reaction time (21 h). At this point, the gel was most degraded and the high charge may be related to oxidation and depolymerization reactions. However, this treatment also drastically decreased the pH of the sample and thus it cannot be fully ruled out that the Na^+ ions from NaOH used to adjust the pH may also have influenced the result.

6.1.5 Discoloration

Yellowing or browning of MFC gels as a consequence of hydrothermal treatment was observed (papers II and IV). Figure 6.4a shows the UV/VIS absorbance of the MFC B at wavelengths of 400-800 nm and the effects of hydrothermal treatment at 150 °C with treatment times of 0-20.5 h. The absorption of the MFC gel increased with increasing hydrothermal treatment time, the greatest change being observed between the untreated sample and sample treated for the shortest time, indicating that the elevated temperature initiated discoloration or structural change relatively rapidly. The increase in light absorption may be due to changes in the particle size (agglomeration) or to chemical changes introducing light-absorbing, functional groups or degradation products.

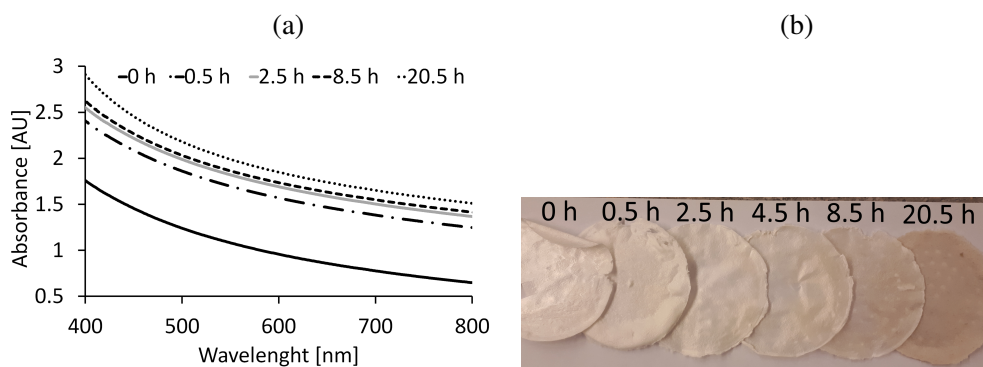


Figure 6.4: (a) UV/VIS absorption spectra of hydrothermally treated MFC gels after hydrothermal treatment at 150 °C. (b) Photographs of dried MFC filter cakes after hydrothermal treatment at 150 °C. The filter cakes were rinsed with ion-exchange water before drying to study whether the discoloration could be removed.

The discoloration of the gels could not be fully removed by rinsing the samples with ion-exchanged water (Figure 6.4b), indicating that some of the chromophoric compounds were partly absorbed or chemically bonded to the fibrils. Table 6.4 presents CIELAB color coordinates (CIE standard illuminant D65 and standard observer 10°), and the brightness of the MFC cakes after they had been rinsed with ion-exchange water and freeze-dried. Hydrothermal treatment increased the yellowness (increasing positive b^* values) and reduced the brightness (decreasing L^* and brightness values). This can also be seen in the photographs of the MFC cakes in Figure 6.4b.

Table 6.4: CIELAB color coordinates (CIE standard illuminant D65 and standard observer 10°) and brightness of the dried MFC cakes.

Sample	L*	a*	b*	Brightness
	D65/10	D65/10	D65/10	R457 D65
0 h	95.72	-0.43	0.68	88.55
0.5 h	94.91	-0.33	1.5	85.61
2.5 h	94.83	-0.26	1.73	85.1
4.5 h	94.1	-0.16	2.28	82.74
8.5 h	92.56	0.34	4.14	77.01
20.5 h	86.61	1.49	6.69	62.06

The surface properties of the dried MFC cakes were measured using XPS and the results are shown in Table 6.5 as atomic percentages of all the samples measured together with the pure cellulose reference specimen.

Table 6.5: XPS (ESCA) surface analysis of dried MFC films after hydrothermal treatment at 150 °C with different times (0-20.5 h). The results are reported as atomic percentages.

Sample	C 1s	O 1s	CC	CO	COO	COOO
0 h	61.9	38.1	9.2	70.9	17.9	2.1
0.5 h	60.2	39.8	5	73.9	19	2.0
2.5 h	61.3	38.7	5.7	73.3	19	2.1
4.5 h	61.9	38.1	5.3	71.9	20.6	2.3
8.5 h	60.5	39.5	3.2	73.4	20.6	2.2
20.5 h	61.2	38.8	5.1	73.9	18.9	2.0
Reference	59.3	40.7	3.8	74.5	19.6	2.0

According to these data, all the treated fibril surfaces consisted only of carbon and oxygen and the high resolution carbon C 1s peaks were all nearly identical with those of the pure cellulose spectrum, with strong C-O and O-C-O features. Thus the analysis showed that the surface of the dried MFC cakes were rather clean with no signs of oxidized surface structure or features that could explain the discoloring. It should be noted that the depth of analysis of XPS is less than 5 nm and that it characterizes only the surface and not the chemical composition of the whole sample, and it is therefore still possible that the chromophoric compounds were inside the matrix rather than on the surface. It has previously been reported that some of the chromophores that may be formed in cellulosic materials by thermal or acidic stresses are highly chromophoric although

they are formed in extremely low quantities and therefore require special methods to be identified (Rosenau et al. 2004, Korntner et al. 2015, Rosenau et al. 2017).

6.1.6 Hydrolysis products

Table 6.6 shows low molar mass sugars, carboxylic acids and furans found in filtrates from hydrothermally treated MFC B (paper IV) as functions of time. Sugars were the main hydrolysis products formed, hemicellulose-derived xylose and xylobiose being the most abundant (Table 6.6). Glucose and cellobiose were also found in the filtrates in small quantities and their presence is probably due to the degradation of cellulose. The amount of sugars clearly increased with longer treatment times. Isomerization products of xylose and glucose, i.e. xylulose and fructose, were identified in the filtrates, showing that isomerization reactions also occur at temperatures as low as 150 °C. Previously xylulose and fructose have been reported after hydrothermal treatment at 160 °C (Lü & Shaka 2012) and at 180 °C (Borrega et al. 2013). The filtrates also contained a number of sugar-type compounds that were only partially characterised.

Numerous organic acids were identified in the filtrates, the amount of each individual acid being low. Formic, glycolic, 3-deoxypentonic (two isomers) and xylonic acids were the most abundant acids. These acids have previously been reported after hydrothermal treatment of xylose and of wood (Oefner et al. 1992, Borrega et al. 2013). Acetic acid was formed only in relatively small quantities, as the deacetylation of hemicelluloses has occurred mostly during the cooking of the pulp. 2-Furancarboxylic acid, 5-formyl-2-furancarboxylic acid and reductic acid, which would have confirmed the degradation of hexenuronic acid groups (Teleman et al. 1996, Sevastyanova et al. 2006b), were not found in the filtrates. The low consistency of MFC (0.99 wt%) during the hydrothermal treatment may mean that some of the degradation products were present in concentrations below the detection limits. Other typical degradation products identified were furfural and 5-HMF that are formed from xylose and glucose respectively by acid-catalyzed dehydration reactions.

Table 6.6: The main sugars, acids and furan compounds found in the filtrates as a function of time after hydrothermal treatment at 150 °C, n.a. = not analyzed tr. = traces and empty cells = not reliably detected.

Compound/Time [h]	Amount mg/g _{MFC}					
	0	0.5	2.5	4.5	8.5	20.5
Carbohydrates						
Xylose	< 0.5	0.5	2.3	3.8	8.1	57.5
Xylulose				tr.	<0.5	1
Glucose		<0.5	<0.5	0.5	0.5	3.1
Fructose					tr.	< 0.5
Other monosaccharides			<0.5	<0.5	<0.5	1.2
Unknown carbohydrates				tr.	<0.5	1
Xylobiose		<0.5	0.8	1.4	3.6	12
Xylotriose		tr	<0.5	<0.5	0.9	1.4
Cellobiose	< 0.5	<0.5	0.5	0.6	<0.5	1.4
Acids						
Formic acid		1.1	1.1	1.4	1.6	2.4
Acetic acid	< 0.5	< 0.5	< 0.5	< 0.5	0.5	0.7
Glycolic acid		< 0.5	0.5	0.5	< 0.5	1.3
Oxalic acid					tr.	< 0.5
Pyruvic acid						< 0.5
Lactic acid			< 0.5	< 0.5	< 0.5	< 0.5
Glyceric acid			< 0.5	< 0.5	< 0.5	< 0.5
2-Hydroxybutanoic acid				tr.	tr.	< 0.5
2,4-Dihydroxybutanoic acid			< 0.5	< 0.5	< 0.5	< 0.5
Threonic acid			< 0.5	< 0.5	tr.	< 0.5
3-Deoxypentonic acid (two isomers)			< 0.5	< 0.5	< 0.5	1.4
3-Deoxyhexonic acid (two isomers)			< 0.5	< 0.5	tr.	0.6
Xylonic acid	< 0.5	< 0.5	< 0.5	< 0.5	< 0.5	0.8
Furans						
Furfural	< 5	n.a.	n.a.	n.a.	< 5	10.3
5-Hydroxymethylfurfural	< 5	n.a.	n.a.	n.a.	< 5	< 5

To gain further information on the main sources of certain identified products, an experiment was carried out using commercial monosaccharides, xylose and glucose, which were exposed to hydrothermal treatment at 150 °C for 20.5 hours, as previously done for MFC, and the non-volatile degradation products were analyzed with GC-MS. A blank experiment (0 h treatment) was included to check the presence of any indigenous impurities in the xylose and glucose starting materials. The xylose material contained small amounts (ca. 1 %) of both pentoses and hexoses. The pentoses clearly contained some arabinose, but some lyxose or more probably ribose may also have been present. In addition, the untreated xylose materials contained some glucose and some other hexoses, apparently galactose and mannose. Xylobiose was also detected in the starting material. The untreated glucose material contained no detectable amounts of pentoses or other hexoses but some hexose disaccharides (probably maltose) were clearly present.

A large number of degradation products were identified or partially characterized after the hydrothermal treatment of glucose and xylose at 150 °C for 20.5 h (Table 6.7). Organic acids formed one of the major compound categories. The C2-C4 hydroxyacids (such as glycolic, lactic and glyceric acids) were formed from both xylose and glucose but the acids with five or six carbon atoms were more selectively formed from the different sugars: levulinic, 2-oxoglutaric and 3-deoxyhexonic acids from glucose and 3-deoxypentonic and xylonic acids from xylose.

Numerous sugar compounds were detected. The most abundant sugars (apart from the starting materials) were isomerization products of both monosaccharides i.e. xylulose (from xylose) and fructose (from glucose). In addition, the filtrates contained several unknown sugar compounds, which were classified based on their mass-spectra and retention times. Sugar-type compounds may include anhydroglucoses (excluding levoglucosan) and sugar-related compounds eluting between mono- and disaccharides indicating that they contain more carbon atoms and hydroxy groups than xylose and glucose and are probably condensation products. Alditol-type and other related compounds were formed especially from xylose, but in the case of glucose their amount was very small. Their mass spectra resembled those of normal alditols, but in each case the spectrum also contained additional, intense ion peaks that are unusual for the trimethylsilylated normal alditols. The disaccharide type sugars and "unusual polyhydroxy compounds" eluted before xylobiose and cellobiose, but they probably contain one sugar unit and another lower fragment unit that remains unknown.

Table 6.7: Degradation/conversion products detected [mg/g_{sugar}] after hydrothermal treatment of xylose and glucose at 150 °C for 20.5 h. N.d. stands for not detected and tr. stands for traces.

Compound or compound category	Xylose	Glucose
Glycolic acid	1.8	1.1
Oxalic acid	<0.5	<0.5
Lactic acid	0.5	<0.5
Pyruvic acid	tr.	tr.
3-Hydroxypropanoic acid	0.5	<0.5
Glyceric acid	0.5	<0.5
2,4-Dihydroxybutanoic acid	<0.5	<0.5
Erythronic acid	<0.5	tr.
Threonic acid	<0.5	tr.
Levulinic acid	n.d.	<0.5
2-Oxoglutaric acid	n.d.	tr.
3-Deoxy- <i>erythro</i> -pentonic acid	1.2	n.d.
3-Deoxy- <i>threo</i> -pentonic acid	2.9	n.d.
Xylonic acid	tr.	n.d.
3-Deoxyhexonic acid (3-4 isomers)	n.d.	5.7
Gluconic acid	n.d.	1.2
Tetroses	tr.	tr.
Xylulose	7	0
Other pentoses	7.1	0.6
Fructose	n.d.	19.8
Other hexoses	0.7	1
Unknown sugar-type compounds	3.9	6.6
Unknown alditol-type compounds	4.7	1.1
Disaccharide-type compounds	0.6	3
Unusual polyhydroxy compounds	0.9	12.7
Reductic acid	1.4	n.d.
5-Hydroxymethylfurfural	n.d.	32.8
2-Furancarboxylic acid	tr.	tr.
Catechol	tr.	tr.
Hydroquinone	n.d.	tr.
Methylcatechol(s)	tr.	tr.
3,4-Dihydroxybenzaldehyde	<0.5	n.d.
Pyrogallol	n.d.	<0.5
1,2,4-Benzenetriol	n.d.	2.7
Benzenetetrol	n.d.	<0.5
3,8-Dihydroxy-2-methylchromone	tr.	n.d.
Unknown aromatic/phenolic compounds	0.5	<0.5

A few cyclic carbohydrate-derived compounds were found. Reductic acid is a known product from pentoses and furfural (Feather & Harris 1973). 5-HMF is a well-known product from the hexose sugars, whereas 2-furancarboxylic acid was found (in trace amounts only) to be formed from both from xylose and glucose.

The existence of possible aromatic compounds was checked by analyzing ether extracts. Trace amounts of catechol, its 3- and 4-methyl derivatives, 3,4-dihydroxy-benzaldehyde, 3,8-dihydroxy-2-methylchromone and at least five other unknown compounds were detected, all formed from xylose. From glucose, the dominating phenolic compound was 1,2,4-benzenetriol which is a well known aromatisation product of 5-HMF (Luijckx et al. 1991). Small amounts of pyrogallol (1,2,3-benzenetriol) were also found, but its route of formation is not clear. In addition, small amounts of a benzenetetrol were formed, but its full structure could not be established.

6.1.7 Effect of pH on rheological properties of non-hydrothermally-treated samples

Because hydrothermal treatment led to acidic degradation products and decreased the pH of the gels, the effect of pH on the rheological properties of MFC was studied. In the experiments, MFC was prepared from enzymatically treated pulp B, but was fluidized only 5 times. The pH of the MFC suspensions were adjusted using 1 M HCl or 1 M NaOH. Figure 6.5a shows the viscosity of MFC as a function of shear rate at three different pH 4.0, 6.5 and 10. At pH 6.5 and 10, the viscosity profiles were similar, but at pH 4 the viscosity decreased. In addition the kink in the viscosity curve shifted to a higher shear rate similarly as was previously observed with hydrothermally treated MFC. A decrease in pH thus seems to explain the observed decrease in viscosity due to hydrothermal treatment. However, in the oscillatory measurements (Figure 6.5b), no increase in storage moduli was observed, indicating that the change in pH does not correlate with the observed increase in storage and loss moduli after hydrothermal treatment and that other mechanisms such as microfibril aggregation should therefore be considered.

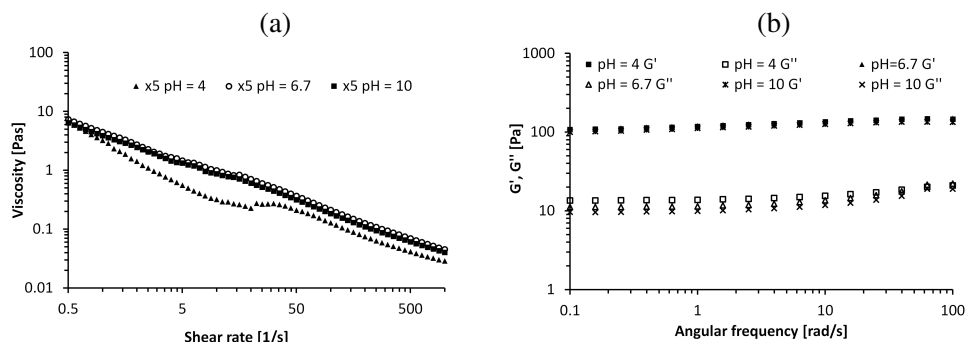


Figure 6.5: (a) Effect of pH on viscosity of MFC gel (fluidized 5 times). Measured at 0.99 wt% consistency. (b) Effect of pH on storage and loss moduli of MFC (fluidized 5 times). Measured at 0.99 wt% consistency using a strain of 0.1%.

Contradictory results concerning the effects of pH on the properties of MFC have previously been reported. Pääkkö et al. (2007) reported an increase in viscosity with decreasing pH with a dilute suspension of MFC prepared from an enzymatically pretreated pulp, and it was suggested that a lower pH enhances interfibrillar interactions by minimizing the effects of repulsive forces between fibrils as the charges are neutralized by the hydrogen ions. On the other hand, Jowkarderis & van de Ven (2014) reported that a lower pH decreased the viscosity of TEMPO-oxidized nanofibrillated cellulose. Agoda-Tandjawa et al. (2010) claimed that the viscoelastic properties of a 1 wt% sugar beet MFC suspension were totally unaffected when the pH was raised from 4.5 to 9. The reasons for the different results are not fully clear, but Agoda-Tandjawa et al. (2010) speculated that part of the difference might be related to the consistency, and that a dilute dispersion of MFC might be influenced more than a concentrated one. It is also probable that the charge density of the MFC grades affects the results.

6.2 Hydrothermal stability of NaCMC

6.2.1 Viscosity

Figure 6.6 shows the viscosity of NaCMC I solutions prepared in deionized water after hydrothermal batch treatment under different conditions (paper I). Untreated NaCMC I solution (Reference, 0.5 wt%) initially showed a shear-thinning flow behavior with a plateau value of zero shear viscosity. After hydrothermal treatment (heated to 118 °C during 150 min) the viscosity decreased and after long-term hydrothermal treatment (at

120 °C during 21 and 45 h) or treatment at high temperature (heated to 158 and 177 °C during 170 and 180 minutes) NaCMC I solutions showed almost Newtonian behavior.

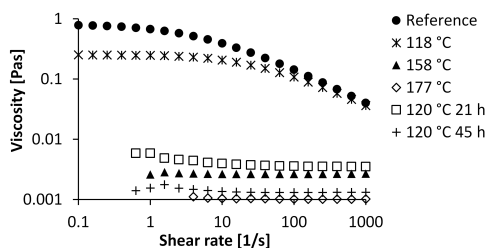


Figure 6.6: Viscosities of NaCMC I solutions measured at 20 °C. Untreated (Reference, 0.5 wt%), heated to 118 °C, 158 °C and 177 °C and after hydrothermal treatment of 21, 45 and 69 hours at 120 °C.

NaCMC solutions often show a shear thinning or pseudoplastic flow behavior but molecular mass, concentration, temperature and salinity are known to affect the rheological properties (Abdelrahim et al. 1994, Clasen & Kulicke 2001, Benchabane & Bekkour 2008). Newtonian or nearly Newtonian behavior of NaCMC solutions at low concentrations has been reported by Ghannam & Esmail (1997) and by Radi & Amiri (2013). After exposure to a high temperature (> 100 °C), a permanent loss of viscosity of NaCMC solutions has been reported (Rao et al. 1981, CP Kelco Oy 2006-2009, Hercules Incorporated 1999), and it is assumed that this is due to heat-initiated depolymerization. If acidic degradation products are formed, the decrease in pH may also affect the result. Chowdhury & Neale (1963) reported that the viscosity of NaCMC solutions had a maximum at around pH 7, because dissociated carboxymethyl groups cause electrostatic repulsion between the similar charges and the NaCMC has a relatively linear conformation. At $\text{pH} < 6$, the viscosity decreases as the charges are protonated which causes a coiling of the NaCMC polymer. In the current study, the pH of the NaCMC solution decreased being 7.0, 7.1, 6.4, 5.6 and 5.3 for untreated, heated to 118 °C and after hydrothermal treatment of 21 h, 45 h and 69 h at 120 °C respectively.

6.2.2 Discoloration

The hydrothermal treatment of NaCMC caused a yellowing or browning of the samples which increased with a higher temperature or longer reaction time. Figure 6.7a presents UV/VIS absorption spectra of hydrothermally treated NaCMC solutions in deionized water treated at 120 °C for 0, 21, 48, and 72 hours. The UV/VIS absorption spectra show

a bimodal structure, in which the first peak was observed at 251-258 nm and the second at 210-220 nm (Figure 6.7a). The observed darkening of the solutions is an indication of a degradation of the cellulose chain, since the colouring of the solutions may be due to the formation of acids or furan compounds (such as 5-HMF). Compounds containing carboxyl or carboxymethyl groups typically have an absorption at ca. 210 nm whereas the optimum absorption of furfurals is at ca. 270 nm. Non-conjugated carbonyl structures generally absorb UV radiation at 270-280 nm (Potthast et al. 2010). The photograph in Figure 6.7b shows the discoloration.

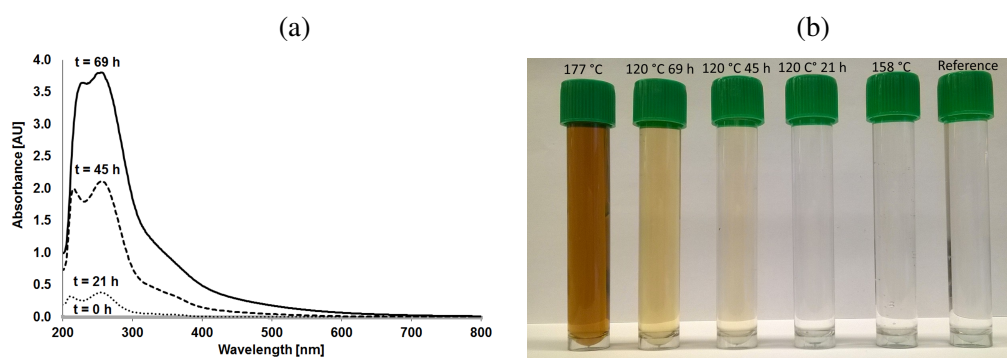


Figure 6.7: (a) UV/VIS absorption spectra of hydrothermally treated NaCMC solutions. (b) Discoloration of NaCMC solutions due to hydrothermal treatment. From the left, heated to 177 °C, 120 °C 69 h, 45 h, 21 h, 158 °C, and no heat treatment.

6.2.3 Surface charge

Table 6.8 shows the charge of the hydrothermally treated NaCMC solutions in deionized water and titrated with two different cationic polymers, PDADMAC and polybrene. It can be seen that the charges of the samples were at approximately the same level (20-25 meq/L) regardless of the cationic titrant used. This shows that both polymers had similar accessibility to NaCMC, which is expected since the anionic charge of the NaCMC creates electrostatic repulsion between the polymers and prevents aggregation. Long-term hydrothermal treatment (45-69 h) at 120 °C reduced the charges of NaCMC polymers only slightly, showing that the negatively charged side groups were rather stable against thermally induced degradation. With a shorter reaction time (118 °C), the opposite was observed. The amount of charged groups increase due to depolymerization and possibly oxidation. A clear decrease in the cationic demand of NaCMC was observed when it was heat treated to 177 °C. At this point, the smallest molecular weight distribution of

NaCMC was observed and the highest amount of acids was detected.

Table 6.8: Charge (meq/L) of NaCMC I. The pH of the samples was adjusted to 6-7 with 0.05 M NaOH.

Treatment	PDADMAC	Polybrene
Reference	21.9	23.5
120 °C 21 h	22.2	24.4
120 °C 45 h	20.2	22.3
120 °C 69 h	17.1	19.6
118 °C	24.2	25.1
137 °C	22.1	24.8
158 °C	22.8	24.2
177 °C	8.5	6.1

The anionic charge of NaCMC polymers originates from a dissociation of carboxymethyl groups. NaCMC is a weak carboxylic acid with a pKa value between 4 and 5 (Thielking & Schmidt 2006, Bakir 2018). The dissociation of the carboxymethyl groups depends largely on the surrounding conditions, especially the pH and salt concentration. In addition, the DS of NaCMC has been found to affect the dissociation. As the DS increases, the distance between the carboxyl groups decreases leading to an increase in the electrostatic interactions, and the dissociation of the carboxyl groups becomes more difficult (Chowdhury & Neale 1963). In general, the chemical stability of the ether bonds in the side groups of carboxymethyl cellulose is strong and the carboxymethyl groups are not easily cleaved by acids (Reese et al. 1950). Typically, the polymer backbone is hydrolyzed before removal of the side groups. Only hot concentrated acids are able to cleave the side groups of NaCMC (Graham 1971). The combined effect of high temperature, high pressure and an increase in the dissociation constant of water at high temperature may possibly be responsible for the observed degradation of the NaCMC I polymer.

6.2.4 Hydrolysis products

Table 6.9 shows the amounts of formic, glycolic and levunic acid and 5-HMF that were detected after hydrothermal treatment of NaCMC I (paper I). When NaCMC I solutions were heated to 118 °C and 137 °C, no acid formation was observed and it is therefore

assumed that the reduction in chain length of NaCMC polymers is the only reaction occurring. At higher temperatures (158 °C) and with long reaction times (21-69 h) at 120 °C, small amounts of glycolic, formic acid and 5-HMF were identified in the filtrates (the amount of degradation products was less than 5 % of the amount of NaCMC). Only the highest applied temperature (177 °C) led to a notable amount of acids. Unknown peaks in the chromatograms were also observed. Sugar-carboxymethyl complexes are likely to occur and other acids may possibly be present. 5-HMF may also possible form condensation products with sugars or acids or 5-HMF itself may resinificate.

Table 6.9: Degradation products [mg/g_{CMC}] from NaCMC I after heating the solutions to temperatures of 118-177 °C and after hydrothermal treatment at 120 °C for 21-69 h. n.d. = not detected.

Sample	Formic acid	Glycolic acid	5-HMF
118 °C	n.d.	n.d.	n.d.
137 °C	n.d.	n.d.	n.d.
158 °C	5.2	5.3	n.d.
177 °C	56.0	197.0	< 5
21 h 120 °C	< 5	< 5	n.d.
45 h 120 °C	16.8	16.8	n.d.
69 h 120 °C	24.8	32.2	tr.

A reduction in chain length of the NaCMC polymer is assumed to be the main reaction occurring during the hydrothermal treatment of NaCMC, as the amount of acids remained low. It was speculated in paper I that glycolic acid could be formed as a degradation product of carboxymethyl groups whereas formic acid and 5-HMF are assumed to be formed as degradation products of glucose. However, based on the experiments with commercial glucose (Table 6.7), all the above-mentioned hydrolysis products including glycolic acid may be formed from glucose. Niemelä & Sjöström (1988) reported that the acid hydrolysis of NaCMC produced significant amount of glucose and glucose-carboxymethyl saccharides but there was no mention of acids detected. This may partly explained that when GC-MS is used for acid analysis, volatile acids such as formic acid cannot be detected. The formation of 5-HMF after 2 minutes hydrothermal treatment of NaCMC at 250 °C has previously been reported by Kröger et al. (2013).

6.3 Short-term steam treatment of NaCMC and MFC

6.3.1 Rheological properties

MFC C and NaCMC II (paper III) were treated hydrothermally at 130 °C with a jet cooker, in which the samples were pumped through a narrow orifice and mixed with hot steam which was injected at a high velocity into the system. The samples were thus exposed to high temperature, high pressure and high shear forces.

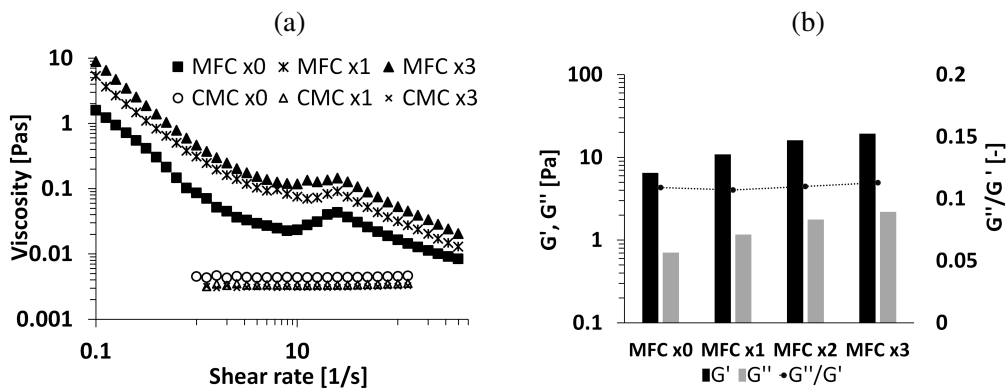


Figure 6.8: (a) Viscosity of MFC C and NaCMC II at a total dry solids content of 0.6 wt% and after 0, 1 and 3 passes through jet cooker at 130 °C (b) Storage (G') and loss moduli (G'') of MFC C passed through jet cooker 0-3 times. Measured with a strain of 1 % and frequency of 1 rad/s.

Figure 6.8a shows the viscosities of the untreated and jet cooked MFC C gels at a total dry content of 0.6 wt%. Jet cooking of the MFC C led to an increase in viscosity with increasing number of passes through the jet cooker. Fig 6.8b shows the storage and loss moduli of the MFC after 0-3 passes through the jet cooker. Both moduli increased with increasing number of passes through the jet cooker, indicating a stronger gel structure. The storage modulus (G') was dominating over the loss modulus (G''), the storage modulus being about 10 times greater than the loss modulus (loss factor ca. 0.1).

The behavior of NaCMC II solution under jet cooking differed from that of MFC C. As shown in Figure 6.8a untreated NaCMC II solution (NaCMC x0) exhibited Newtonian behavior in which the viscosity did not depend on the shear rate, due to the relatively low degree of polymerization and the low concentration of NaCMC, and the NaCMC solutions had no elastic properties. After exposure to high temperature (130 °C) combined

with shear forces under jet cooking, the viscosity of the NaCMC solutions (NaCMC x1, NaCMC x3) decreased slightly.

There is little information in the literature about the effects of short-term high-temperature steam treatments on MFC or on NaCMC. The increase in viscosity and storage and loss moduli after exposure of MFC C to jet cooking are assumed to occur due to the exposure to shear forces, as the samples pass through the narrow orifice. This may cause cutting and further fibrillation of coarse MFC that affects the rheology. The surface area measurements supported this hypothesis, as the surface area was noticed to increase with the passes through the jet cooker (paper III). In the case of NaCMC II, the slight decrease in viscosity may be due to a decrease in the chain length of the polymer due to the high temperature and high shear forces. The pH of NaCMC solutions remained practically constant ($\text{pH} \approx 7.5$) after the steam treatment.

6.3.2 Short-term steam-treatment tests with MFC/NaCMC Mix

A mixture containing 50 wt% of MFC C and 50 wt% of NaCMC II was treated in the jet cooker. Figure 6.9a shows the viscosities of the MFC/NaCMC blends before and after jet cooking at a dry solids content of 0.6 wt%. A shear thinning behavior was observed for this mixture, showing that the MFC dominated the viscosity over the NaCMC. After 1 and 3 passes through the jet cooker, the viscosity of the MFC/NaCMC mixture was very close to the value for MFC alone, although the concentrations of MFC and NaCMC in the mixture were 0.3 wt% and NaCMC alone showed a much smaller viscosity.

With oscillatory measurements, the opposite behavior was observed, because the storage and loss moduli of the MFC/NaCMC mixture were lower than those of MFC alone. The storage modulus of the MFC/NaCMC mix was about six times greater than the loss modulus (loss factor 0.17-0.18) whereas that of MFC alone was about ten times greater (loss factor around 0.1). The higher liquid-like property is probably due to the presence of NaCMC and the smaller amount of MFC (0.3 wt%) than in the pure MFC suspension.

It has previously been reported (with non-hydrothermally-treated samples) that NaCMC has a dispersing effect on MFC (Ahola et al. 2008, Sorvari et al. 2014) and that the viscosity of a MFC/NaCMC mixture was higher than that of MFC alone (Sorvari et al. 2014). Therefore, the dispersing effects of NaCMC probably explain the relatively high viscosities of MFC/NaCMC mix also in this study. The dispersing effect increased with increasing passes through the jet cooker, possibly because the jet cooker enabled an

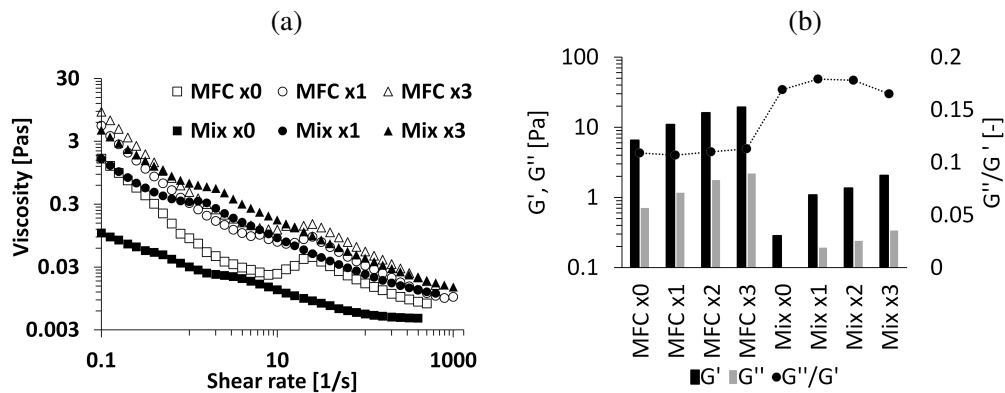


Figure 6.9: (a) Viscosities of MFC/NaCMC mix (50/50 wt%) at a total dry solids content of 0.6 wt% (the amount of each individual component in the MFC/NaCMC mixture being 0.3 wt%) after 0, 1 and 3 passes through jet cooker. (b) Storage (G') and loss moduli (G'') MFC/NaCMC mix passed through jet cooker 0-3 times. Measured with a strain of 1 % and frequency of 1 rad/s.

efficient mixing of the material and NaCMC increased the delamination of unfibrillated fiber fragments and dispersed flocs. Sorvari et al. (2014) also reported that the gel strength diminished compared to that of pure MFC, probably because the NaCMC reduced the contact between the fibrils. This result is also consistent with the current study.

7 Conclusions

In this study, hydrothermal stability of MFC has been studied with different methods to clarify the strength of a cellulose gel network and to determine hydrothermally induced changes in physicochemical properties of MFC gel. Rheological properties, water-retention, surface charge and UV/VIS absorption spectra of MFC gels before and after hydrothermal treatment were determined. The ability of MFC to resist thermal hydrolysis and decomposition was estimated by determining the low molar mass sugars, organic acids and furan compounds in the filtrates.

It was found that MFC gel goes through molecular and supramolecular changes when exposed to hydrothermal treatment, the viscosity being reduced, but MFC prepared from endoglucanase-pretreated dissolving pulp showed promising results, as the viscosity of the gel was not greatly affected even after hydrothermal treatment at 120 °C for 21 h or at 150 °C for 7.5 h under batch conditions. The storage and loss moduli increased with moderate hydrothermal treatment indicating a stiffening of the gel network by aggregation, which may be due to hydrolysis of the charged groups or to a structural reorganization. It should be noted that different measuring parameters showed different effects of hydrothermal treatment, a reduction in water retention capacity and an increase in UV-absorption spectra being observed already after the shortest treatment times in the batch experiments, showing the sensitivity of the MFC towards these parameters. The analysis of low molar mass degradation products in filtrates revealed that numerous degradation products were formed but the amounts of individual compounds were low. Hydrolysis reactions led to isomerization products of sugars and hydroxyacids that are common in alkaline conditions and, on the other hand, the formation of furfural and 5-HMF that are associated with acid-catalyzed reactions. Aromatic compounds were also formed from simple sugars under hydrothermal treatment and they have an effect on the sample discoloration.

In the experiments carried out with NaCMC solutions, the viscosity was found to decrease and this was confirmed in both batch and dynamic experiments. Sample discoloration after hydrothermal treatment was also observed with NaCMC solutions, but based on polyelectrolyte titration, carboxymethyl groups had a good stability against hydrothermal treatment. A MFC/NaCMC mixture showed promising results when exposed to short-term hydrothermal treatment as the viscosities of MFC/NaCMC mixture were relatively high compared to that of MFC alone, probably due to dispersing effect of NaCMC.

However, the storage and loss moduli and gel-like behavior of MFC/NaCMC mix were less than that of MFC alone. Short-term steam treatment did not weaken the rheological properties of this system.

The results obtained in this work have increased the knowledge on hydrothermally induced changes on physicochemical properties of MFC. This information is essential when exploiting the applicability of MFC to different uses. The analysis of the filtrates provided information on the by-products that is essential to product safety aspects.

References

- Abdelrahim, K. A., Ramaswamy, H. S., Dyon, G. & Toupin, C. (1994), 'Effects of concentration and temperature on carboxymethylcellulose rheology', *International Journal of Food Science and Technology* **29**, 243–253.
- Abdelrahim, K. & Ramaswamy, H. (1995), 'High temperature/pressure rheology of carboxymethyl cellulose (CMC)', *Food Research International* **28**(3), 285–290.
- Agoda-Tandjawa, G., Durand, S., Berot, S., Blassel, C., Gaillard, C., Garnier, C. & Doublier, J.-L. (2010), 'Rheological characterization of microfibrillated cellulose suspensions after freezing', *Carbohydrate Polymers* **80**(3), 677–686.
- Ahola, S., Myllytie, P., Österberg, M., Teerinen, T. & Laine, J. (2008), 'Effect of polymer adsorption on cellulose nanofibril water binding capacity and aggregation', *Bioresources* **3**, 1315–1328.
- Aida, T. M., Shiraishi, N., Kubo, M., Watanabe, M. & Smith Jr, R. L. (2010), 'Reaction kinetics of D-xylose in sub- and supercritical water', *Journal of Supercritical Fluids* **55**, 208–216.
- Alén, R. (2011), 'Cellulose derivatives', in *'Biorefining of Forest Resources'*, Vol. 20, Paper Engineers' Association, Espoo, pp. 305–354.
- Alén, R. (2015), 'Chapter 3A - Pulp mills and wood-based biorefineries', in *'Industrial Biorefineries & White Biotechnology'*, Elsevier, Amsterdam, pp. 91–126.
- Arola, S., Malho, J.-M., Laaksonen, P., Lille, M. & Linder, M. B. (2013), 'The role of hemicellulose in nanofibrillated cellulose networks', *Soft Matter* **9**, 1319–1326.
- Bakir, T. (2018), 'Apparent dissociation constant of cellulose gum acid', *Asian Journal of Chemistry* **30**, 1019–1022.
- Beamson, G. & Briggs, D. (1992), *High Resolution XPS of Organic Polymers: the Scienta ESCA300 Database*, John Wiley & Sons, Ltd, Chichester.
- Benchabane, A. & Bekkour, K. (2008), 'Rheological properties of carboxymethyl cellulose (CMC) solutions', *Colloid and Polymer Science* **286**, 1173–1180.
- Beyer, M., Koch, H. & Fischer, K. (2006), 'Role of hemicelluloses in the formation of chromophores during heat treatment of bleached chemical pulps', *Macromolecular Symposia* **232**, 98–106.
- Bobleter, O. (1994), 'Hydrothermal degradation of polymers derived from plants', *Progress in Polymer Science* **19**, 797–841.
- Borrega, M., Concha-Carrasco, S., Pranovich, A. & Sixta, H. (2017), 'Hot water treatment of hardwood kraft pulp produces high-purity cellulose and polymeric xylan', *Cellulose* **24**, 5133–5145.

- Borrega, M., Niemelä, K. & Sixta, H. (2013), 'Effect of hydrothermal treatment intensity on the formation of degradation products from birchwood', *Holzforschung* **67**, 871–879.
- Borrega, M., Nieminen, K. & Sixta, H. (2011), 'Degradation kinetics of the main carbohydrates in birch wood during hot water extraction in a batch reactor at elevated temperatures', *BioResource Technology* **102**, 10724–10732.
- Borrega, M. & Sixta, H. (2015), 'Water prehydrolysis of birch wood chips and meal in batch and flow-through systems: A comparative evaluation', *Industrial & Engineering Chemistry Research* **54**(23), 6075–6084.
- Cancela, M., Álvarez, E. & Maceiras, R. (2005), 'Effects of temperature and concentration on carboxymethylcellulose with sucrose rheology', *Journal of Food Engineering* **71**, 419–424.
- Cao, X., Peng, X., Sun, S., Zhong, L., Chen, W., Wang, S. & Sun, R.-C. (2015), 'Hydrothermal conversion of xylose, glucose, and cellulose under the catalysis of transition metal sulfates', *Carbohydrate Polymers* **118**, 44 – 51.
- Chatterjee, A. & Das, B. (2013), 'Radii of gyration of sodium carboxymethylcellulose in aqueous and mixed solvent media from viscosity measurement', *Carbohydrate Polymers* **98**(2), 1297–1303.
- Chirat, C. & De La Chapelle, V. (1999), 'Heat- and light-induced brightness reversion of bleached chemical pulps', *Journal of Pulp and Paper Science* **25**, 201–205.
- Chowdhury, F. H. & Neale, S. M. (1963), 'Acid behavior of carboxylic derivatives of cellulose. Part I. Carboxymethylcellulose', *Journal of Polymer Science: Part A* **1**, 2881–2891.
- Clasen, C. & Kulicke, W.-M. (2001), 'Determination of viscoelastic and rheo-optical material functions of water-soluble cellulose derivatives', *Progress in Polymer Science* **26**(9), 1839–1919.
- Conner, A. H. (1984), 'Kinetic modeling of hardwood prehydrolysis. Part I. Xylan removal by water prehydrolysis', *Wood and Fiber Science* **16**, 268–277.
- Cowie, J., Bilek, E., Wegner, T. H. & Shatkin, J. A. (2014), 'Market projections of cellulose nanomaterial-enabled products - Part 2: Volume estimates', *Tappi* **13**, 57–69.
- CP Kelco Oy (2006-2009), 'Carboxymethylcellulose (CMC) book'. 1st edition.
- deButts, E. H., Hudy, J. A. & Elliott, J. H. (1957), 'Rheology of sodium carboxymethylcellulose solutions', *Industrial and Engineering Chemistry* **49**, 94–98.
- Ding, Q., Zenga, J., Wang, B., Tanga, D., Chena, K. & Gao, W. (2019), 'Effect of nanocellulose fiber hornification on water fraction characteristics and hydroxyl accessibility during dehydration', *Carbohydrate Polymers* **207**, 44–51.

- Diniz, J. F., Gil, M. & Castro, J. (2004), 'Hornification-its origin and interpretation in wood pulps', *Wood Science and Technology* **37**, 489–494.
- Eyholzer, C., Bordeanu, N., Lopez-Suevos, F., Rentsch, D., Zimmermann, T. & Oksman, K. (2010), 'Preparation and characterization of water-redispersible nanofibrillated cellulose in powder form', *Cellulose* **17**(1), 19–30.
- Fahlén, J. & Salmén, L. (2003), 'Cross-sectional structure of the secondary wall of wood fibers as affected by processing', *Journal of Materials Science* **38**(1), 119–126.
- Feather, M. & Harris, J. (1973), 'Dehydration reactions of carbohydrates', *Advances in Carbohydrate Chemistry and Biochemistry* **28**, 161–224.
- Forsskåhl, I., Tylli, H. & Olkkonen, C. (2000), 'Participation of carbohydrate-derived chromophores in the yellowing of high-yield and TCF pulps', *Journal of Pulp and Paper science* **26**, 245–249.
- Garrote, G., Domínguez, H. & Parajó, J. C. (1999), 'Hydrothermal processing of lignocellulosic materials', *Holz als Roh- und Werkstoff* **57**, 191–202.
- Gehlen, M. H. (2010), 'Kinetics of autocatalytic acid hydrolysis of cellulose with crystalline and amorphous fractions', *Cellulose* **17**(2), 245–252.
- Ghannam, M. T. & Esmail, M. N. (1997), 'Rheological properties of carboxymethyl cellulose', *Journal of Applied Polymer Science* **64**(2), 289–301.
- Gómez-Díaz, D. & Navaza, J. M. (2003), 'Rheology of aqueous solutions of food additives effect of concentration, temperature and blending', *Journal of Food Engineering* **56**, 387–392.
- Gondo, T., Watanabe, M., Soma, H., Kitao, O., Yanagisawa, M. & Isogai, A. (2006), 'Sec-mals study on carboxymethyl cellulose (cmc): Relationship between conformation of cmc molecules and their adsorption behavior onto pulp fibers', *Nordic Pulp and Paper Research Journal* **21**, 591–597.
- Graham, H. D. (1971), 'Determination of carboxymethylcellulose in food products', *Journal of Food Science* **36**, 1052–1055.
- Granström, A., Eriksson, T., Gellersted, G., Rööst, C. & Larsson, P. (2001), 'Variables affecting the thermal yellowing of TCF-bleached birch kraft pulps', *Nordic Pulp & Paper Research Journal* **16**, 18–23.
- Gullón, P., Romani, A., Vila, C., Garrote, G. & Parajó, J. C. (2012), 'Potential of hydrothermal treatments in lignocellulose biorefineries', *Biofuels, Bioproducts and Biorefining* **6**(2), 219–232.
- Heggset, E. B., Chinga-Carrasco, G. & Syverud, K. (2017), 'Temperature stability of nanocellulose dispersions', *Carbohydrate Polymers* **157**, 114–121.

- Helmerius, J., Vinblad von Walter, J., Rova, U., Berglund, K. A. & Hodge, D. B. (2010), 'Impact of hemicellulose pre-extraction for bioconversion on birch kraft pulp properties', *Bioresource Technology* **101**, 5996–6005.
- Hercules Incorporated (1999), 'Aqualon sodium carboxymethylcellulose Physical and Chemical Properties', Hercules Plaza, Wilmington.
- Herric, F., Casebier, R., Hamilton, J. & Sandberg, K. (1983), 'Microfibrillated cellulose: Morphology and accessibility', *Journal of Applied Polymer Science: Applied Polymer Symposium* **37**, 797–813.
- Iotti, M., Gregersen, Ø. W., Moe, S. & Lenes, M. (2011), 'Rheological studies of microfibrillar cellulose water dispersions', *Journal of Polymers and the Environment* **19**(1), 137–145.
- Iwamoto, S., Nakagaito, A. N. & Yano, H. (2007), 'Nano-fibrillation of pulp fibers for the processing of transparent nanocomposites', *Applied Physics A* **89**, 461–466.
- Iwamoto, S., Nakagaito, A., Yano, H. & Nogi, M. (2005), 'Optically transparent composites reinforced with plant fiber-based nanofibers', *Applied Physics A* **81**, 1109–1112.
- Johansson, L.-S. & Campbell, J. M. (2004), 'Reproducible XPS on biopolymers: cellulose studies.', *Proceedings of the 10th European Conference on Applications of Surface and Interface Analysis* **36**, 1018–1022.
- Johnson, R. K., Zink-Sharp, A., Renneckar, S. H. & Glasser, W. G. (2009), 'A new bio-based nanocomposite fibrillated tempo-oxidized celluloses in hydroxypropylcellulose matrix', *Cellulose* **16**(2), 227–238.
- Jowkarderis, L. & van de Ven, T. G. M. (2014), 'Intrinsic viscosity of aqueous suspensions of cellulose nanofibrils', *Cellulose* **21**(4), 2511–2517.
- Junka, K., Filpponen, I., Lindström, T. & Laine, J. (2013), 'Titrimetric methods for the determination of surface and total charge of functionalized nanofibrillated/microfibrillated cellulose (NFC/MFC)', *Cellulose* **20**, 2887–2895.
- Karppinen, A., Saarinen, T., Salmela, J., Laukkanen, A., Nuopponen, M. & Seppälä, J. (2012), 'Flocculation of microfibrillated cellulose in shear flow', *Cellulose* **19**(6), 1807–1819.
- Kato, K. L. & Cameron, R. E. (1999), 'A review of the relationship between thermally-accelerated ageing of paper and hornification', *Cellulose* **6**, 23–40.
- Khaled, B. & Abdelbaki, B. (2012), 'Rheological and electrokinetic properties of carboxymethylcellulose-water dispersions in the presence of salts', *International Journal of Physical Sciences* **9**, 1790–1798.

- Khalil, H. A., Davoudpour, Y., Islam, M. N., Mustapha, A., Sudesh, K., Dungani, R. & Jawaidd, M. (2014), 'Production and modification of nanofibrillated cellulose using various mechanical processes: A review', *Carbohydrate Polymers* **99**, 649–665.
- Kibblewhite, R. P. & Hamilton, K. A. (1984), 'Fibre cross-section dimensions of undried and dried pinus radiata kraft pulps', *New Zealand Journal of Forestry Science* **14**, 319–330.
- Klemm, D., Cranston, E. D., Fischer, D., Gama, M., Kedzior, S. A., Kralisch, D., Kramer, F., Kondo, T., Lindström, T., Nietzsche, S., Petzold-Welcke, K. & Rauchfuß, F. (2018), 'Nanocellulose as a natural source for groundbreaking applications in materials science: Today's state', *Materials Today* **21**(7), 720–748.
- Kontturi, E. & Vuorinen, T. (2009), 'Indirect evidence of supramolecular changes within cellulose microfibrils of chemical pulp fibers upon drying', *Cellulose* **16**, 65–74.
- Korntner, P., Hosoya, T., Dietz, T., Eibinger, K., Reiter, H., Spitzbart, M., Röder, T., Borgards, A., Kreiner, W., Mahler, A. K., Winter, H., Groiss, Y., French, A. D., Henniges, U., Potthast, A. & Rosenau, T. (2015), 'Chromophores in lignin-free cellulosic materials belong to three compound classes. Chromophores in celluloses, XII', *Cellulose* **22**, 1053–1062.
- Kröger, M., Hartmann, F. & Klemm, M. (2013), 'Hydrothermal treatment of carboxymethyl cellulose salt: Formation and decomposition of furans, pentenes and benzenes', *Chemical Engineering & Technology* **36**, 287–294.
- Lahtinen, P., Liukkonen, S., Pere, J., Sneck, A. & Kangas, H. (2014), 'A comparative study of fibrillated fibers from different mechanical and chemical pulps', *BioResources* **9**, 2115–2127.
- Laine, J. & Stenius, P. (1997), 'Effect of charge on the fibre and paper properties of bleached industrial kraft pulps', *Paper and Timber* **79**, 257–266.
- Lavoine, N., Desloges, I., Dufresne, A. & Bras, J. (2012), 'Microfibrillated cellulose its barrier properties and applications in cellulosic materials: A review', *Carbohydrate Polymers* **90**(2), 735–764.
- Lindström, T., Naderi, A. & Wiberg, A. (2015), 'Large scale applications of nanocellulosic materials - a comprehensive review -', *Journal of Korea Technical Association of The Pulp and Paper Industry* **47**, 5–21.
- Lojewska, J., Missoriand, M., Lubanska, A., Grimaldi, P., Zieba, K., Proniewicz, L. M. & Castellano, A. C. (2007), 'Carbonyl groups development on degraded cellulose. Correlation between spectroscopic and chemical results', *Applied Physics A* **89**, 883–881.

- Lopez, C. G., Rogers, S. E., Colby, R. H., Graham, P. & Cabral, J. T. (2015), 'Structure of sodium carboxymethyl cellulose aqueous solutions: A SANS and rheology study', *Journal of Polymer Science, Part B: Polymer Physics* **53**, 492–501.
- Lorand, E. J. (1939), 'Preparation of cellulose ethers', *Industrial & Engineering Chemistry* **31**, 891–897.
- Lowys, M.-P., Desbrières, J. & Rinaudo, M. (2001), 'Rheological characterization of cellulosic microfibril suspensions. Role of polymeric additives', *Food Hydrocolloids* **15**(1), 25 – 32.
- Lü, X. & Shaka, S. (2012), 'New insights on monosaccharides' isomerization, dehydration and fragmentation in hot compressed water', *The Journal of Supercritical Fluids* **61**, 146–456.
- Luijkx, G. C., van Rantwijk, F., van Bekkum, H. & Antal Jr, M. J. (1995), 'The role of deoxyhexonic acids in the hydrothermal decarboxylation of carbohydrates', *Carbohydrate Research* **272**, 191–202.
- Luijkx, G., van Rantwijk, F. & van Bekkum, H. (1991), 'Formation of 1,2,4-benzenetriol by hydrothermal treatment of carbohydrates', *Recueil des Travaux Chimiques des Pays-Bas* **110**, 343–344.
- Lyytikäinen, K., Saukkonen, E., Kajanto, I. & Käyhkö, J. (2011), 'The effect of hemicellulose extraction on fiber charge properties and retention behaviour of kraft pulp fibers', *BioResources* **6**, 219–231.
- Maloney, T. (2015), 'Network swelling of TEMPO-oxidized nanocellulose', *Holzforschung* **69**, 207–213.
- Naderi, A. & Lindström, T. (2016), 'A comparative study of the rheological properties of three different nanofibrillated cellulose systems', *Nordic Pulp & Paper Research Journal* **31**, 354–363.
- Naderi, A., Lindström, T., Erlandsson, J., Sundström, J. & Flodberg, G. (2016), 'A comparative study of the properties of three nano-fibrillated cellulose systems that have been produced at about the same energy consumption levels in the mechanical delamination step', *Nordic Pulp & Paper Research Journal* **31**, 364–371.
- Nechyporchuk, O., Belgacem, M. N. & Bras, J. (2016), 'Production of cellulose nanofibrils: A review of recent advances', *Industrial Crops and Products* **93**, 2–25.
- Niemelä, K. (1990), 'The formation of hydroxy monocarboxylic acids and dicarboxylic acids by alkaline thermochemical degradation of cellulose', *Journal of Chemical Technology & Biotechnology* **48**, 17–28.
- Niemelä, K. & Sjöström, E. (1986), 'The conversion of cellulose into carboxylic acids by a drastic alkali treatment', *Biomass* **11**, 215–221.

- Niemelä, K. & Sjöström, E. (1988), 'Identification of the products of hydrolysis of carboxymethylcellulose', *Carbohydrate Research* **180**, 43–52.
- Notley, S. M. (2008), 'Effect of introduced charge in cellulose gels on surface interactions and the adsorption of highly charged cationic polyelectrolytes', *Physical Chemistry Chemical Physics* **10**, 1819–1825.
- Nsor-Atindana, J., Chen, M., Goff, H. D., Zhong, F., Sharif, H. R. & Li, Y. (2017), 'Functionality and nutritional aspects of microcrystalline cellulose in food', *Carbohydrate Polymers* **172**, 159 – 174.
- Oefner, P. J., Lanziner, A. H., Bonn, G. & Bobleter, O. (1992), 'Quantitative studies on furfural and organic acid formation during hydrothermal, acidic and alkaline degradation of D-xylose', *Monatshefte für Chemie / Chemical Monthly* **123**(6), 547–556.
- Olszewska, A., Eronen, P., Johansson, L.-S., Malho, J.-M., Ankerfors, M., Lindström, T., Ruokolainen, J., Laine, J. & Österberg, M. (2011), 'The behaviour of cationic nanofibrillar cellulose in aqueous media', *Cellulose* **18**(5), 1213–1226.
- Pääkkö, M., Ankerfors, M., Kosonen, H., Nykänen, A., Ahola, S., Österberg, M., Ruokolainen, J., Laine, J., Larsson, P. T., Ikkala, O. & Lindström, T. (2007), 'Enzymatic hydrolysis combined with mechanical shearing and high-pressure homogenization for nanoscale cellulose fibrils and strong gels', *Biomacromolecules* **8**(6), 1934–1941.
- Pääkkönen, T., Dimic-Misic, K., Orelma, H., Pönni, R., Vuorinen, T. & Maloney, T. (2016), 'Effect of xylan in hardwood pulp on the reaction rate of TEMPO-mediated oxidation and the rheology of the final nanofibrillated cellulose gel', *Cellulose* **23**, 277–293.
- Plaza, M. & Turner, C. (2015), 'Pressurized hot water extraction of bioactives', *Trends in Analytical Chemistry* **71**, 39–54.
- Pönni, R., Kontturi, E. & Vuorinen, T. (2013), 'Accessibility of cellulose: Structural changes and their reversibility in aqueous media', *Carbohydrate Polymers* **93**(2), 424–429.
- Pönni, R., Vuorinen, T. & Kontturi, E. (2012), 'Proposed nano-scale coalescence of cellulose in chemical pulp fibers during technical treatments', *BioResources* **7**, 6077–6108.
- Potthast, A., Rosenau, T. & Kosma, P. (2010), *Polysaccharides II*, Springer.
- Quivy, N., Jacquet, N., Sclavons, M., Deroanne, C., Paquot, M. & Devaux, J. (2010), 'Influence of homogenization and drying on the thermal stability of microfibrillated cellulose', *Polymer Degradation and Stability* **95**(3), 306–314. Special Issue: MoDeSt 2008.

- Radi, M. & Amiri, S. (2013), 'Comparison of the rheological behavior of solutions and formulated oil-in-water emulsions containing carboxymethylcellulose (CMC)', *Journal of Dispersion Science and Technology* **34**(4), 582–589.
- Rao, M. A., Walter, R. H. & Cooley, H. J. (1981), 'Effect of heat treatment on the flow properties of aqueous guar gum and sodium carboxymethylcellulose (CMC) solutions', *Journal of Food Science* **46**(3), 896–899.
- Rasmussen, H., Sørensen, H. R. & Meyer, A. S. (2014), 'Formation of degradation compounds from lignocellulosic biomass in the biorefinery: sugar reaction mechanisms', *Carbohydrate Research* **385**, 45–57.
- Reese, E., Siu, R. & Levins, H. (1950), 'The biological degradation of soluble cellulose derivatives and its relationship to the mechanism of cellulose hydrolysis', *Journal of Bacteriology* **59**, 485–497.
- Rosenau, T., Potthast, A., Milacher, W., Hofinger, A. & Kosma, P. (2004), 'Isolation and identification of residual chromophores in cellulosic materials', *Polymer* **45**, 6437–6443.
- Rosenau, T., Potthast, A., Zwirchmayr, N. S., Hettegger, H., Plasser, F., Hosoya, T., Bacher, M., Krainz, K. & Dietz, T. (2017), 'Chromophores from hexeneuronic acids: identification of HexA-derived chromophores', *Cellulose* **24**(9), 3671–3687.
- Saarikoski, E., Saarinen, T., Salmela, J. & Seppälä, J. (2012), 'Flocculated flow of microfibrillated cellulose water suspensions: an imaging approach for characterisation of rheological behaviour', *Cellulose* **19**, 647–659.
- Saito, T., Kimura, S., Nishiyama, Y. & Isogai, A. (2007), 'Cellulose nanofibers prepared by TEMPO-mediated oxidation of native cellulose', *Biomacromolecules* **8**, 2485–2491.
- Salmén, L. & Stevanic, J. S. (2018), 'Effect of drying conditions on cellulose microfibril aggregation and "hornification"', *Cellulose* **25**, 6333–6344.
- Sandoval-Torres, S., Jomaa, W., Marc, F. & Puiggali, J.-R. (2010), 'Causes of color changes in wood during drying', *Forestry Studies in China* **12**, 167–175.
- Sevastyanova, O., Li, J. & Gellersted, G. (2006a), 'Influence of various oxidizable structures on the brightness stability of fully bleached chemical pulps', *Nordic Pulp & Paper Research Journal* **21**, 49–53.
- Sevastyanova, O., Li, J. & Gellersted, G. (2006b), 'On the reaction mechanism of the thermal yellowing of bleached chemical pulps', *Nordic Pulp & Paper Research Journal* **21**, 188–192.
- Shafiei-Sabet, S., Martinez, M. & Olson, J. (2016), 'Shear rheology of micro-fibrillar cellulose aqueous suspensions', *Cellulose* **23**(5), 2943–2953.

- Shatkin, J. A., Wegner, T. H., Bilek, E. & Cowie, J. (2014), 'Market projections of cellulose nanomaterial-enabled products- Part 1: Applications.', *TAPPI Journal* **13**, 9–16.
- Silveira, R. L., Stoyanov, S. R., Kovalenko, A. & Skaf, M. S. (2016), 'Cellulose aggregation under hydrothermal pretreatment conditions', *Biomacromolecules* **17**(8), 2582–2590.
- Siro, I. & Plackett, D. (2010), 'Microfibrillated cellulose and new nanocomposite materials: a review', *Cellulose* **17**, 459–494.
- Siró, I., Plackett, D., Hedenqvist, M., Ankerfors, M. & Lindström, T. (2011), 'Highly transparent films from carboxymethylated microfibrillated cellulose: The effect of multiple homogenization steps on key properties', *Journal of Applied Polymer Science* **119**, 2652–2660.
- Sjöström, E. (1989), 'The origin of charge on cellulosic fibers', *Nordic Pulp & Paper Research Journal* **4**, 90–93.
- Song, T., Pranovich, A. & Holmbom, B. (2012), 'Hot-water extraction of ground spruce wood of different particle size', *BioResources* **7**, 4214–4225.
- Sorvari, A., Saarinen, T., Haavisto, S. & Salmela, J. (2014), 'Modifying the flocculation of microfibrillated cellulose suspension by soluble polysaccharides under conditions unfavorable to adsorption', *Carbohydrate Polymers* **106**, 283–292.
- Spence, K. L., Venditti, R. A., Rojas, O. J., Habibi, Y. & Pawlak, J. J. (2010), 'The effect of chemical composition on microfibrillar cellulose films from wood pulps: water interactions and physical properties for packaging applications', *Cellulose* **17**, 835–848.
- Srokol, Z., Bouche, A.-G., van Estrik, A., Strik, R. C., Maschmeyer, T. & Peters, J. A. (2004), 'Hydrothermal upgrading of biomass to biofuel; studies on some monosaccharide model compounds', *Carbohydrate Research* **339**(10), 1717–1726.
- Stigsson, V., Kloow, G., Germgård, U. & Andersson, N. (2005), 'The influence of cobalt (II) in carboxymethyl cellulose processing', *Cellulose* **12**, 395–401.
- Teleman, A., Harjunpää, V., Tenkanen, M., Buchert, J., Hausalo, T., Drakenberg, T. & Vuorinen, T. (1995), 'Characterisation of 4-deoxy- β -l-threo-hex-4-enopyranosyluronic acid attached to xylan in pine kraft pulp and pulping liquor by ^1H in and ^{13}C NMR spectroscopy', *Carbohydrate Research* **272**, 55–71.
- Teleman, A., Hausalo, T., Tenkanen, M. & Vuorinen, T. (1996), 'Identification of the acidic degradation products of hexenuronic acid and characterisation of hexenuronic acid-substituted xylooligosaccharides by NMR spectroscopy', *Carbohydrate Research* **280**, 197–208.

- Theander, O. & Nelson, D. A. (1988), 'Aqueous, high-temperature transformation of carbohydrates relative to utilization of biomass', *Advances in Carbohydrate Chemistry and Biochemistry* **46**, 273–326.
- Thielking, H. & Schmidt, M. (2006), 'Cellulose Ethers', in *Ullmann's Encyclopedia of Industrial Chemistry*, Wiley-VCH Verlag GmbH & Co. KGaA Weinheim, pp. 381–397.
- Thomas, D. C. (1982), 'Thermal stability of starch and carboxymethyl cellulose-based polymers used in drilling fluids', *Society of Petroleum Engineers Journal* **22**, 171–180.
- Tingaut, P., Zimmermann, T. & Lopez-Suevos, F. (2010), 'Synthesis and characterization of bionanocomposites with tunable properties from poly(lactic acid) and acetylated microfibrillated cellulose', *Biomacromolecules* **11**(2), 454–464.
- Trache, D., Hussin, M. H., Chuin, C. T. H., Sabar, S., Fazita, M. N., Taiwo, O. F., Hassan, T. & Haafiz, M. M. (2016), 'Microcrystalline cellulose: Isolation, characterization and bio-composites application - A review', *International Journal of Biological Macromolecules* **93**, 789 – 804.
- Vuorinen, T., Buchert, J., Teleman, A., Tenkanen, M. & Fagerström, P. (1996), Selective hydrolysis of hexenuronic acid groups and its application in ECF and TCF bleaching of kraft pulps, in *'International Pulp Bleaching Conference Proceedings, Washington D.C., 14.-18.4.1996. TAPPI, 1996. p. 43-51.'*
- Vuorinen, T. J., Buchert, J., Teleman, A. B.-L. & Tenkanen, M. (2004), 'Method of treating cellulosic pulp to remove hexenuronic acid Patent No.: US 6776876 B1'.
- Wang, J., Gardner, D. J., Stark, N. M., Bousfield, D. W., Tajvidi, M. & Cai, Z. (2018), 'Moisture and oxygen barrier properties of cellulose nanomaterial-based films', *ACS Sustainable Chemistry & Engineering* **6**(1), 49–70.
- Weise, U. (1998), 'Hornification - mechanisms and terminology', *Paper and Timber* **80**, 110–115.
- Welf, E., Venditti, R. A., Hubbe, M. A. & Pawlak, J. J. (2005), 'The effects of heating without water removal and drying on the swelling as measured by water retention value and degradation as measured by intrinsic viscosity of cellulose papermaking fibers', *Progress in Paper Recycling* **14**, 1–9.
- Wüstenberg, T. (2015), *Cellulose and Cellulose Derivatives in the Food Industry - Fundamentals and Applications*, Wiley VCH Verlag GmbH & Co. KGaA.
- Yang, X. H. & Zhu, W. (2007), 'Viscosity properties of sodium carboxymethylcellulose solutions', *Cellulose* **14**, 409–417.
- Yoshida, K., Kusaki, J., Ehara, K. & Saka, S. (2005), 'Characterization of low molecular weight organic acids from beech wood treated in supercritical water', *Applied Biochemistry and Biotechnology* **123**, 795–806.

Publication I

Hiltunen, S., Chunlin, C., Willför, S. & Backfolk, K.
**Thermally induced degradation of NaCMC in water and effects of
NaHCO₃ on acid formation and charge**

Reprinted with permission from
Food Hydrocolloids,
Vol. 74C, pp. 32-36, 2018
© 2018 Elsevier.

The final publication is available at
<https://doi.org/10.1016/j.foodhyd.2017.07.028>

Publication II

Hiltunen, S., Heiskanen, I. & Backfolk, K.

**Effect of hydrothermal treatment of microfibrillated cellulose on
rheological properties and formation of hydrolysis products**

Reprinted with permission from
Cellulose

Vol. 25, issue 8, pp. 4653-4662, 2018

© 2018 Springer Science and Business Media.

The final publication is available at
<https://doi.org/10.1007/s10570-018-1884-2>

Publication III

Hiltunen, S., Heiskanen, I. & Backfolk, K.

**Short-term steam treatment of MFC gel with and without
water-soluble cellulose derivative**

Reprinted with permission from
Nordic Pulp & Paper Research Journal

Vol. 34, issue 1, pp. 10-18, 2019

© 2019 De Gruyter

The final publication is available at
<https://doi.org/10.1515/npprj-2018-0062>

Publication IV

Hiltunen, S., Koljonen, K., Niemelä, K., Heiskanen, I., Johansson, L.-S. &
Backfolk, K.

**Hydrothermally induced changes in properties of MFC and
characterization of the low-molar mass degradation products**

Accepted to Cellulose

The final publication is available at
<https://doi.org/10.1007/s10570-019-02603-w>

ACTA UNIVERSITATIS LAPPEENRANTAENSIS

- 827. RANAEI, SAMIRA. Quantitative approaches for detecting emerging technologies. 2018. Diss.
- 828. METSO, LASSE. Information-based industrial maintenance - an ecosystem perspective. 2018. Diss.
- 829. SAREN, ANDREY. Twin boundary dynamics in magnetic shape memory alloy Ni-Mn-Ga five-layered modulated martensite. 2018. Diss.
- 830. BELONOGOVA, NADEZDA. Active residential customer in a flexible energy system - a methodology to determine the customer behaviour in a multi-objective environment. 2018. Diss.
- 831. KALLIOLA, SIMO. Modified chitosan nanoparticles at liquid-liquid interface for applications in oil-spill treatment. 2018. Diss.
- 832. GEYDT, PAVEL. Atomic Force Microscopy of electrical, mechanical and piezo properties of nanowires. 2018. Diss.
- 833. KARELL, VILLE. Essays on stock market anomalies. 2018. Diss.
- 834. KURONEN, TONI. Moving object analysis and trajectory processing with applications in human-computer interaction and chemical processes. 2018. Diss.
- 835. UNT, ANNA. Fiber laser and hybrid welding of T-joint in structural steels. 2018. Diss.
- 836. KHAKUREL, JAYDEN. Enhancing the adoption of quantified self-tracking wearable devices. 2018. Diss.
- 837. SOININEN, HANNE. Improving the environmental safety of ash from bioenergy production plants. 2018. Diss.
- 838. GOLMAEI, SEYEDMOHAMMAD. Novel treatment methods for green liquor dregs and enhancing circular economy in kraft pulp mills. 2018. Diss.
- 839. GERAMI TEHRANI, MOHAMMAD. Mechanical design guidelines of an electric vehicle powertrain. 2019. Diss.
- 840. MUSIIENKO, DENYS. Ni-Mn-Ga magnetic shape memory alloy for precise high-speed actuation in micro-magneto-mechanical systems. 2019. Diss.
- 841. BELIAEVA, TATIANA. Complementarity and contextualization of firm-level strategic orientations. 2019. Diss.
- 842. EFIMOV-SOINI, NIKOLAI. Ideation stage in computer-aided design. 2019. Diss.
- 843. BUZUKU, SHQIPE. Enhancement of decision-making in complex organizations: A systems engineering approach. 2019. Diss.
- 844. SHCHERBACHEVA, ANNA. Agent-based modelling for epidemiological applications. 2019. Diss.
- 845. YLIJOKI, OSSU. Big data - towards data-driven business. 2019. Diss.
- 846. KOISTINEN, KATARIINA. Actors in sustainability transitions. 2019. Diss.

847. GRADOV, DMITRY. Experimentally validated numerical modelling of reacting multiphase flows in stirred tank reactors. 2019. Diss.
848. ALMPANOPOULOU, ARGYRO. Knowledge ecosystem formation: an institutional and organisational perspective. 2019. Diss.
849. AMELI, ALIREZA. Supercritical CO₂ numerical modelling and turbomachinery design. 2019. Diss.
850. RENEV, IVAN. Automation of the conceptual design process in construction industry using ideas generation techniques. 2019. Diss.
851. AVRAMENKO, ANNA. CFD-based optimization for wind turbine locations in a wind park. 2019. Diss.
852. RISSANEN, TOMMI. Perspectives on business model experimentation in internationalizing high-tech companies. 2019. Diss.
853. HASSANZADEH, AIDIN. Advanced techniques for unsupervised classification of remote sensing hyperspectral images. 2019. Diss.
854. POPOVIC, TAMARA. Quantitative indicators of social sustainability applicable in process systems engineering. 2019. Diss.
855. RAMASAMY, DEEPIKA. Selective recovery of rare earth elements from diluted aqueous streams using N- and O –coordination ligand grafted organic-inorganic hybrid composites. 2019. Diss.
856. IFTEKHAR, SIDRA. Synthesis of hybrid bio-nanocomposites and their application for the removal of rare earth elements from synthetic wastewater. 2019. Diss.
857. HUIKURI, MARKO. Modelling and disturbance compensation of a permanent magnet linear motor with a discontinuous track 2019. Diss.
858. AALTO, MIKA. Agent-based modeling as part of biomass supply system research. 2019. Diss.
859. IVANOVA, TATYANA. Atomic layer deposition of catalytic materials for environmental protection. 2019. Diss.
860. SOKOLOV, ALEXANDER. Pulsed corona discharge for wastewater treatment and modification of organic materials. 2019. Diss.
861. DOSHI, BHAIRAVI. Towards a sustainable valorisation of spilled oil by establishing a green chemistry between a surface active moiety of chitosan and oils. 2019. Diss.
862. KHADIJEH, NEKOUJIAN. Modification of carbon-based electrodes using metal nanostructures: Application to voltammetric determination of some pharmaceutical and biological compounds. 2019. Diss.
863. HANSKI, JYRI. Supporting strategic asset management in complex and uncertain decision contexts. 2019. Diss.
864. OTRA-AHO, VILLE. A project management office as a project organization's strategizing tool. 2019. Diss.



ISBN 978-952-335-401-2
ISBN 978-952-335-402-9 (PDF)
ISSN-L 1456-4491
ISSN 1456-4491
Lappeenranta 2019